CODEN:LUTEDX/(TEIE-5461)/1-66/(2021)

IndustrialElectricalEngineeringandAutomation

Harmonic Emissions in Microgrids

A Case Study of Simris

Lejla Alibegovic

Emelie Freiland Paulsson

Division of Industrial Electrical Engineering and Automation

Faculty of Engineering, Lund University

MASTER THESIS

Harmonic Emissions in Microgrids

A Case Study of Simris

Lejla Alibegovic
Emelie Freiland Paulsson

Supervisors
Neil Hancock, E.ON
Olof Samuelsson, IEA

Examiner
Morten Hemmingsson, IEA

Faculty of engineering LTH

Division of Industrial Electrical Engineering and Automation, IEA

June 7, 2021

Abstract

This work aimed to analyse current and voltage harmonics in a microgrid where the purpose was to examine if harmonics behave differently in grid-connected mode and island mode and if there is a correlation between weather and harmonics. The purpose was also to see if electrical harmonics can be reproduced in a model of the microgrid in a simulation program and what the limitations of such a simulation are.

The microgrid studied was developed by E.ON and contains a wind turbine, photovoltaic panels, a backup generator, battery energy system and loads. The microgrid was disconnected from the distribution grid at limited times during the project. This thesis work was limited to only having the wind turbine and PV panels as harmonic sources. In order to develop this work, the method chosen was to analyse collected microgrid data for various measurement points and weather conditions and then construct a model based on this live system data.

The data analysis showed constant current harmonic emission levels independent of the wind speed and irradiation, except for the fifth harmonic at the PV installation. It also showed that the harmonic levels were higher for grid-connected mode than for island mode. The simulated harmonics were smaller than the measured harmonics and therefore, they could not be reproduced in the simulation model.

There is no general correlation between weather and harmonic emission levels. The harmonics were higher in grid-connected mode as the harmonics from the distribution grid are added to the microgrid. The simulation was based on only harmonics from the wind turbine and photovoltaic panels. However, the real microgrid has several sources of harmonic emission, which make the measured harmonic values higher than the simulated values.

Key words: *Local energy system, Microgrid, Harmonics, Renewable energy sources, NEPLAN*

Acknowledgements

We would like to express our utmost gratitude towards our LTH supervisor, Professor Olof Samuelsson, for your continuous support, motivation, advice and sharing your knowledge with us. We would also like to thank Doctoral Student Imran Maqbool for sharing your expertise with us and for guiding us throughout the simulation and calculation process.

Further we would like to thank the Business development department at E.ON Energidistribution in Malmö for giving us the opportunity to write this thesis and for welcoming us and giving us valuable advice. A special thank you goes out to our supervisor at E.ON, Neil Hancock, for your time, engagement and support. We appreciate you showing us the microgrid in Simris and sharing your knowledge about it and project management with us. Furthermore we would like to extend our gratitude to Ola Ivarsson for sharing your knowledge, information and contacts with us.

Additionally we would like to give a special thank you to Professor Math Bollen for giving us invaluable insight into the field of harmonics and taking his time to discuss the subject with us.

Finally, we would want to express our utmost gratitude to our parents for their encouragement, support, and guidance during both this endeavor and our education.

Malmö, June 2021
Lejla Alibegovic
Emelie Freiland Paulsson

List of Abbreviations

AC - Alternating Current
BESS - Battery Energy System Storage
BUG - Backup Generator
DC - Direct Current
DSR - Demand Side Response
HD - Harmonic Distortion
LES - Local Energy System
LV - Low Voltage
MPP - Maximum Power Point
MV - Medium Voltage
PV - Photovoltaic
PWM - Pulse Width Modulation
RES - Renewable Energy Source
RMS - Root Mean Square
THD - Total Harmonic Distortion
WT - Wind Turbine
WTG - Wind Turbine Generator

Contents

1 Introduction

This section presents the background and motivation for the thesis. The purpose, limitations and previous work on the topic are also given in this section.

1.1 Background and Motivation

"Affordable and clean energy" is EUs 7th Sustainable Development Goal and includes an increase of renewable energy generation in the global energy mix [1]. A lot of the responsibility falls on the energy sector to transform and obtain solutions for a more sustainable future. The development is going towards decreased decentralized generation and an increased share of renewable energy sources(RES) like wind- and solar power. This requires new network systems and technologies with added flexibility and capacity. The power system needs to change to adapt to increased electricity usage, urbanization and decreased share of large generation [2]. The "bottleneck effect" is evident in many areas where the generation is sufficient, but the grid does not have the capacity to deliver enough power to certain cities or regions. The network reinforcements that are needed for a continuous, stable and secure power supply are an enormous expense, which drives interest in alternatives such as small-scaled renewable generation [3].

Many challenges arise with the shift to decentralized generation with weather-dependent RES. There is also an increased environmental engagement from customers, which makes local energy systems (LES), also called microgrids, one candidate for the future type of energy system. A "Local energy system (LES) is a climate-friendly self-supporting energy ecosystem serving the energy needs (electricity, hot water and space heating) for a customer, or a group of customers, through local energy sources" [2]. This thesis will use the term microgrid instead of LES as we are only looking at electricity. The microgrid can be disconnected from the distribution grid and operate on its own during outages, compensate for network reinforcement and be cost-effective in remote areas [2].

Power quality, including harmonics, is a known issue with the new devices for electricity usage and production. RES are connected to the grid through switching power electronic converters, which are the primary source for harmonics if the correct filters are not used. New usage patterns with converter-based loads also affect the harmonics content in the grid. Many benefits can be gained with good power quality [4]. Harmonics include voltage and current waveform deviations from the ideal sinusoidal wave with a 50 Hz fundamental frequency [5]. A grid with a large number of harmonics can cause broken components, overheating and ageing, leading to an increased risk for power failure [4]. In 1997 the Swedish government issued a law called Ellag (1997:857), which states that all transmission and distribution of electricity must be of good quality. It also states that the owners of the distribution network shall correct deficiencies if it is reasonable in relation to the inconveniences [6]. This means that bad power quality with high levels of harmonics is unacceptable.

E.ON has implemented Sweden's first local energy system provided by 100% renewable energy as a part of the EU project InterFlex that aims to explore different smart grid technologies. The microgrid is located in the small village Simris (149 households) outside Simrishamn in southern Sweden [7]. It is supplied with a wind turbine, photovoltaic (PV) panels, a battery energy system storage (BESS), a backup generator (BUG) and a demand-side response (DSR) system [8]. At limited times during the project's duration (2017-2020), the microgrid is operated in island mode, which means that it got disconnected from the distribution grid [7]. The Simris LES case study aims to gain more knowledge about power quality in microgrids with only renewable energy generation. During islanding, there is 100% converter-based production from wind and solar power, which are sources of harmonic emissions. This makes harmonics in microgrids interesting when the network shifts between island operation and regular operation to ensure good electric power quality.

1.2 Purpose and Research Questions

The purpose of this thesis is to analyse the power quality in Simris microgrid, more specifically, voltage and current harmonic emissions. Furthermore, it aims to analyze on site collected data and investigate if reproduced simulations of harmonics in the microgrid can be made with the simulation program NEPLAN. The research questions are presented below.

- What is the relation between harmonics from renewable energy sources in the Simris microgrid and the weather?
- How do electrical harmonics distinguish in grid-connected mode and island mode?
- Is it possible to make a valid model of Simris in the simulation program NEPLAN?

1.3 Limitations

This study is limited to a specific case, the Simris microgrid, focusing on harmonics from the renewable energy source: wind and solar power. Other possible sources of harmonics are not included but briefly discussed. The main focus is to study the harmonics in the microgrid and not deeper investigate the why and how harmonics are distinguished in a specific way. Three monitoring points were analysed to limit the amount of data. 10-minute average values for odd harmonics in the first phase will be studied. This means that even harmonics will not be studied as they are negligibly small or nonexistent in the electric power system [9]. The collected data was limited to the 15th harmonic order, and therefore this thesis is limited to frequencies in the range of 50-750 Hz. This means that harmonics from PWM(several kHz) in the wind turbine/PV-park will not be included in this work.

1.4 Previous Work

Harmonics in the power grid is a well-known topic for grid owners and has been investigated in different aspects over the last 20 years. Harmonics in the Simris microgrid are less well understood, so this report is built on knowledge from previous work applied to this specific case.

In a study [10] presented harmonic voltage distortion in a single house microgrid, with 22.6 kWp solar PV installation. Both individual and total harmonic distortion (THD) were examined in island mode and grid-connected mode. It showed that microgrids in most cases have a higher voltage THD in island operation than when it is connected to the grid. It also showed that the highest values of the voltage distortion correspond to instances during the night with low load and in island operation [10].

Harmonic simulations have been presented in some papers, where one paper used the simulation program Pspice Circuit Simulator and the harmonic were validated within an error of 5 %. They proved that the simulations could provide relatively accurate results if the input parameters are well-known [11].

One report addresses harmonic emissions from wind power and that those emissions can be amplified from resonances in the grid [12]. A report from Energiforsk was studying harmonics spread from wind turbines to the public grid and harmonics spread between the wind turbines. The conclusion was that harmonics from wind turbines are small but amplified by resonances due to the capacitance in long cables[13]. In another report, harmonic emission measurements from individual wind turbines and a wind power plant (WPP) were studied. The harmonic emission in the percentage of the rating was low, and no connection between production and the harmonic level was found [14].

The issue of having a limit on the amount of PV generation that can be connected to the 12 kV grid due to harmonic resonances is analysed in a report. The inverter connecting the PV panels to the grid creates harmonics that are amplified by large capacitors in the substations. The paper analyses the issue and identify different ways the problem could be solved [15]. Another report studies harmonics

and supraharmonic emissions in the 2-150 kHz range from PV-installations and LED lamps. The study showed that the emissions from PV were generally low and varying for different powers. Different harmonic emission spectrum for low order harmonics was found for different PV manufactures [16] likely because of different converters.

2 Local Energy Systems

An introduction to microgrids and specifically the microgrid in Simris, with its topology and grid components, is presented in the section.

2.1 Microgrids

Traditionally, power is generated in centralized power plants and transferred via the high voltage grid. Today there is an increased penetration of generation in the low voltage(LV) and medium voltage(MV) grid. The power flow is no longer just one-directional but multidirectional with generation from RES at both private households and other owners. This transition comes with the interest of creating smaller local energy grids, so-called microgrids, with their own control system [17] containing small-scale production that can support the microgrid on rare occasions its own. With a microgrid, it is possible to utilize weather-based production by having a control system that regulates the demand against the generation, which creates a more effective intelligent energy system [17]. This is an important development with economic and environmental benefits for the future.

Islanding is when the microgrid is disconnected from the distribution grid and operates autonomously. Having a balance between supply and load is crucial to maintain island grid stability, as imbalance will cause frequency fluctuations and increase the risk for grid failure. The power quality and system stability will be affected negatively from fluctuations in the frequency [18]. To balance the microgrid in island mode, the generation, loads and battery system are interconnected. Renewable energy generation cannot be connected to the grid without inverters/converters that are known to introduce problems in the microgrid [19], which will be explained further in section 3.5. There are still many challenges and knowledge to gain about microgrids, and it is a hot topic within the power supply companies today.

2.2 Simris Microgrid

The renewable energy in the Simris microgrid is produced by a single wind turbine (WT) and a solar power system of PV panels. There are some customers with private solar cells connected to the microgrid. A lithium-ion and redox-flow battery are used to store excess energy necessary when the energy generation is insufficient for the customers' demand. The system also has a backup generator(BUG) that is mainly used during islanding. It is more economical to use the distribution grid to back up the grid when the system is not islanding. An energy management system controls the connected grid and is the center of the system. The grid topology of Simris is shown in figure 1 and component information is found in table 1 [8].

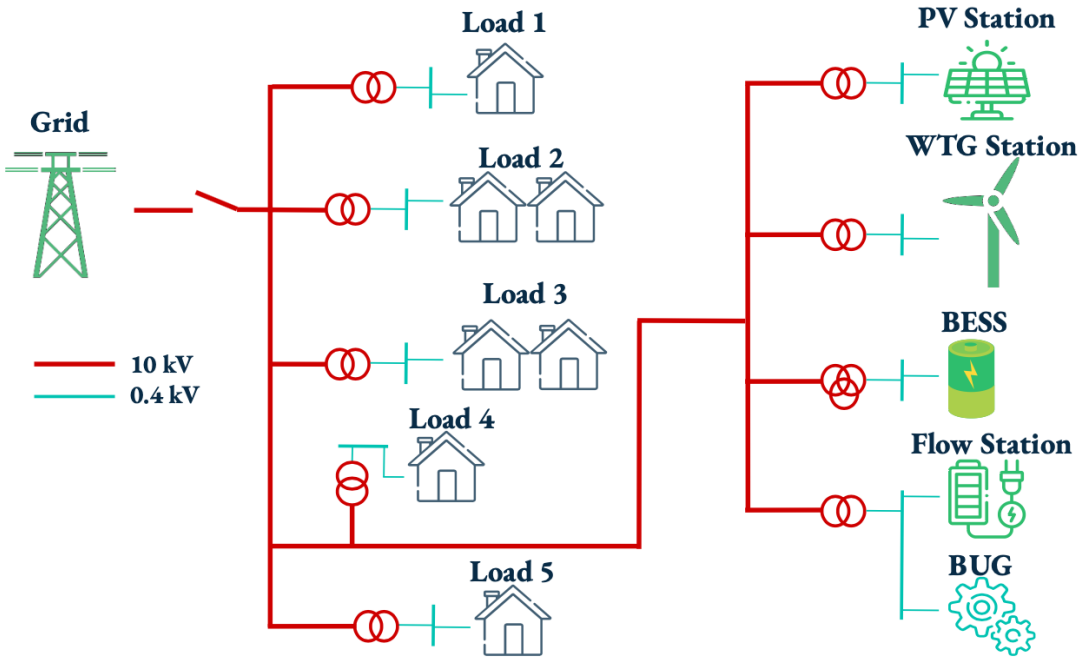

Figure 1: Topology of Simris microgrid, where the red lines represents the MV grid, 10kV, and the blue line presents the LV grid, 0.4kV.

The microgrid is connected to the distribution grid, where the management system manages the connection. The microgrid was disconnected from the distribution grid and operated in island mode once every five weeks throughout the duration of the project. A conventional circuit breaker was used to make the transition. In island mode, the aim was to maintain the frequency, voltage and power quality in a zero inertia power system. Regulation of the grid was made digitally with the battery system and with the demand system response. EON controlled household assets like heat pumps, hot tap water boilers, residential batteries and PV installations to regulate the local energy system [3].

Table 1: Information about the components in Simris

Component	Power (kW)	Energy
Solar PV	440	0.45 GWh/a
Wind turbine	500	1.5 GWh/a
Lithium-ion battery	800	0.33 MWh
Redox Flow battery	200	1.2 MWh
Backup generator	480	-
Households	800	2.1 GWh/a

2.2.1 PV Installation

The solar park, installed in 2013, is around 3000 m^2 with a maximum power of 440 kW and consists of type Sunmodule SW 245 Poly with maximum power at 245 Wp at irradiation of $1000W/m^2$, 25°C and AM 1.5. There are 60 polycrystalline cells per module [20], meaning that they are blended from multiple pieces of silicon.

The inverters used with the solar panels are called Sunny Tripower, and they are multi-string inverters.

Each inverter converts the direct current (DC) of a PV array into alternating current (AC) [21]. The maximal power point (MPP) tracker samples the output of the PV cells and applies the required load to achieve maximum power for any given environmental conditions [22]. By using pulse width modulation(PWM) switching, the inverter converts from DC to AC, generating high-frequency harmonics. The inverters used are equipped with filters to limit the THD value [21].

2.2.2 Wind Turbine

The WT in Simris was installed in 1996 and is an Enercon E-40/6.44 with a rated power of 500kW, which is reached at 12m/s. The cut-in wind speed is 2.5 m/s and the cut-out wind speed is 25 m/s [23]. The WT has a low-speed synchronous generator that is not directly connected to the grid, allowing variable speed. The wind energy converters in the turbine are equipped with a grid management system which consists of a rectifier, DC link and modular inverter system. The current, voltage and frequency are continuously recorded to ensure that the produced power is properly fed into the grid [24]. The WT has an "inertia emulation property" that stores the kinetic energy in the rotor blades to compensate for an energy drop and give a more stable generation [24].

2.2.3 Battery

The Simris battery system consists of two different kinds of batteries. The first battery is a lithium-ion battery capable of fast response and is powerful, but a full discharge or many deep discharge cycles are expected to shorten the battery's effective lifetime. As such, it utilises a 60-70 % charge/discharge cycle window. In Simris, this battery is connected to the 0.7kV grid with an inverter that is then connected to the 0.4kV grid. The battery works as a regulator of fast changes in frequency. The Li-ion battery and its associated battery management system is also to as BESS [3].

The Vanadium-redox-Flow Energy Storage-System is from the company Enerox of type CellCube FB 250-1000 R3. It has a rated power of 250kW and contains 1MWh energy. The battery is connected to the 0.4 kV grid and function as a buffer for baseload during a longer time period. The technology behind the battery is that the energy is stored in two tanks with vanadium electrolysis in different oxidation states. The electrolysis is pumped through serial connected cell stacks that are divided by a membrane that only allows the exchange of ions. The applied voltage decides if the battery is charged or discharged. The electrochemical process consists of vanadium changing states, and no electrolyte is consumed over time. This gives the battery a plus 20 years lifetime and a 100% discharge cycle without any harm to the battery. Another advantage of a flow battery is that the energy tank and power output are decoupled. If more energy is needed, a bigger tank can be added. The flow battery technology installed acts more slowly than the lithium battery and is as such better suited for management of base power during a long time [25].

2.2.4 Measurement Equipment

Different measurement or power analysis equipment are used depending on the aim of the measurement. When the absolute limit is essential for disputes, inspections, educational studies, or such, the measurement equipment used must fully meet the IEC 61000-4-30, class A requirements. If the measurements instead are taken for troubleshooting the system, simpler equipment can be used. So all measurements do not need the highest standard. It has been shown that some parameters are very hard to measure where one of these is harmonics [26].

Metrum PQ120 and Janitza UMG604 are two different power analysers that are installed in the microgrid in Simris. Metrum is fulfilling the class A requirements for harmonics [27] and Janitza is not reaching the class A requirements for harmonics [28]. The effect of this is considered so small that it should not make a difference for the purpose of our project.

3 Harmonic Theory

This section presents the theory and definitions related to harmonics, voltage harmonic guidelines and harmonic emissions from renewable energy sources and loads.

In an AC power system, the perfect current should be an ideal sinusoidal wave of the fundamental frequency 50 Hz in the Swedish power system. "Waveform distortion includes all deviations of the voltage or current waveform from the ideal sine wave"[5]. The definition is closely related to voltage- and current quality. Voltage quality has to do with "how the network affects the load", while current quality is "how the load affects the network" [29]. Harmonic distortion (HD), harmonic emission or simply harmonics are one kind of waveform distortion which is a power quality issue.

Different aspects of electric power quality has received much attention and there are many reasons to the increased importance and some of them are [5]:

- More current disturbances are produced by equipment.
- Equipment, production processes and companies have become less tolerant to disturbances.
- Renewable energy generation creates new power quality issues.

The Swedish Energy Markets Inspectorate (EI) has determined regulations that distribution network operators must follow to ensure good electric power quality. One of the main topics is voltage quality which includes harmonic distortion [30]. As the main topic of this report is harmonics, it will be described further in the following part.

3.1 Harmonic Distortion

Harmonic distortion is when the voltage or current "waveform is nonsinusoidal but periodic with a period of one cycle"(50 Hz). The waveform contains harmonic components that are multiple integers of the fundamental frequency [5]. Frequencies up to 2 kHz are referred to as harmonics and higher frequencies (2-150 kHz) is called supraharmonics [16] and will not be in focus in this thesis. The consequences of distortion include more significant losses and overheating. Increased frequency gives an increased "heating effect", especially in series components. Heavily distorted signals will damage components in the electrical system or electronic equipment [5].

3.1.1 The Fourier analysis

The waveform with harmonics distortion can be represented by the Fourier series, which is an infinite sequence of sine and cosine waves [31]. The Fourier analysis is used to study frequencies and form a relationship between a function in the time domain and a function in the frequency domain. Fourier's theorem states that every nonsinusoidal periodic waveform can be decomposed as the sum of sine waves through the application of the Fourier series. Fourier series results from calculating both the magnitude and phase of the fundamental frequency and the harmonics of the periodic waveform. To represent the Fourier series of a periodic function x(t) in the frequency domain, equation 1 is used. Where a_0 is the average value of x(t), T is the period and a_n and b_n are coefficients that can be calculated using equations 2 and 3 [32].

$$x(t) = \frac{a_0}{2} + \sum_{n=1}^{\infty} a_n cos(2\pi \frac{nt}{T}) + b_n sin(2\pi \frac{nt}{T}) \tag{1}$$

$$a_n = \frac{2}{T}\int_0^T x(t)cos(2\pi\frac{nt}{T})dt \tag{2}$$

$$b_n = \frac{2}{T}\int_0^T x(t)sin(2\pi\frac{nt}{T})dt \tag{3}$$

3.1.2 Odd harmonics

The odd harmonics are more common and observable in the power system because the load current waveforms have half-wave symmetry [9]. Half-wave symmetry means that the second half of the wave is precisely opposite to the first half and the wave is symmetrical around the origin. This can be seen in figure 2, where the sine wave represents the half-wave symmetry. Thus, the distortion's effect is the same for the positive and negative half of the sinusoidal wave [5].

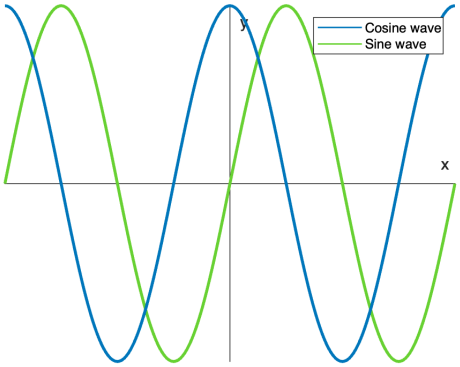

Figure 2: Represents the symmetry of odd harmonics, sine wave in green, and even harmonics, cosine wave in blue.

Odd current and voltage harmonics that are multiples of third harmonics (3rd, 9th, 15th, etc.) are called triplen harmonics. Balanced triplen harmonics are zero sequence in nature since their phase quantity has the same magnitude and phase angle [33]. Triplen harmonics increase the current in the system faster than other harmonics and are therefore less desired. In a paper written by Grady [34] he explains that Steinmetz proposed using delta connections in transformers to block the third harmonic currents. A transformer generally has a wye connection on the LV side and a delta connection on the MV side. In a wye-connection, see figure 3, the current form A, B and C are summed at N (neutral).

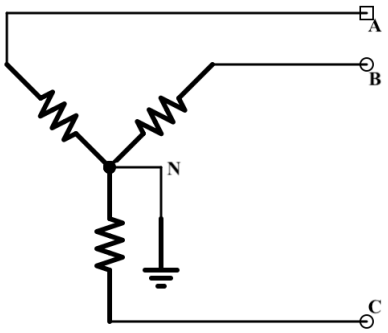

Figure 3: A wye connection.

This means that 3rd harmonics will be three times bigger whilst the fundamental current will be zero. The proof of this concept can be seen in equations 4-7, were equations 4-6 represent the phase currents containing the 1st and 3rd harmonics. Equation 7 represents the neutral point where all the phase currents are added. It can be seen that only the 3rd harmonic is left after summing them together, therefore a wye-wye transformer cannot be used to decrease or block triplen harmonics.

$$i_A(t) = i_1 sin(\omega t) + i_3 sin(3\omega t) \tag{4}$$

$$i_B(t) = i_1 sin(\omega t - 120^\circ) + i_3 sin(3(\omega t - 120)) = i_1 sin(\omega t - 120^\circ) + i_3 sin(3\omega t) \tag{5}$$

$$i_C(t) = i_1 sin(\omega t + 120^\circ) + i_3 sin(3(\omega t + 120^\circ)) = i_1 sin(\omega t + 120^\circ) + i_3 sin(3\omega t) \tag{6}$$

$$\begin{aligned} i_N(t) = i_A(t) + i_B(t) + i_C(t) &= i_1 sin(\omega t) + i_1 sin(\omega t - 120^\circ) + i_1 sin(\omega t + 120^\circ) \\ &+ i_3 sin(3\omega t) + i_3 sin(3\omega t) + i_3 sin(3\omega t) = i_1 sin(\omega t) - \frac{1}{2} i_1 sin(\omega t) + \frac{\sqrt{3}}{2} i_1 cos(\omega t) \\ &- \frac{1}{2} i_1 sin(\omega t) - \frac{\sqrt{3}}{2} i_1 cos(\omega t) + 3 i_3 sin(3\omega t) = 3 i_3 sin(3\omega t) \end{aligned} \tag{7}$$

In a perfectly balanced system the currents have a phase difference of 120°. Meaning that in a transformer with a delta connection the third harmonics are in opposition and will therefor neutralize each other. The proof of this concept can be seen in equation 8-11 below [35]. Figure 4 shows a delta connection and there is no neutral point.

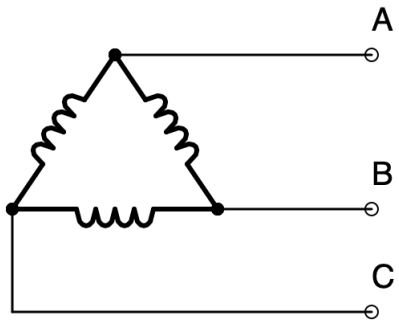

Figure 4: A delta connection.

The phase magnetising currents i_A, i_B and i_c are of the following form, where its assumed that each non-linear load will only contain the 1st, 3rd and 5th harmonic components of current.

$$i_A(t) = i_1 sin(\omega t) + i_3 sin(3\omega t) + i_5 sin(5\omega t) \tag{8}$$

$$\begin{aligned} i_B(t) &= i_1 sin(\omega t - 120^\circ) + i_3 sin(3(\omega t - 120)) + i_5 sin(5(\omega t - 120^\circ)) \\ &= i_1 sin(\omega t - 120^\circ) + i_3 sin(3\omega t) + i_5 sin(5(\omega t - 120^\circ)) \end{aligned} \tag{9}$$

$$\begin{aligned} i_C(t) &= i_1 sin(\omega t + 120^\circ) + i_3 sin(3(\omega t + 120^\circ)) + i_5 sin(5(\omega t + 120^\circ)) \\ &= i_1 sin(\omega t + 120^\circ) + i_3 sin(3\omega t) + i_5 sin(5(\omega t + 120^\circ)) \end{aligned} \tag{10}$$

From equation 8, 9 and 10 it can be seen that third harmonic in the three-phase currents have the same phase. As the line current in a delta connection is the difference between two-phase currents, the third harmonic current is not present in the line current, which can be seen in equation 11. Therefore no third harmonic current will exit past the transformer with a delta winding in a balanced system, as it circulates the closed-loop of the delta [35].

$$\begin{aligned} i_{AB}(t) = i_A(t) - i_B(t) &= i_1 sin(\omega t) - i_1 sin(\omega t - 120^\circ) + i_3 sin(3\omega t) \\ &- i_3 sin(3\omega t) + i_5 sin(5\omega t) - i_5 sin(5(\omega t - 120^\circ)) \\ &= i_1(\frac{3}{2} sin(\omega t) + \frac{\sqrt{3}}{2} cos(\omega t)) + i_5(\frac{3}{2} sin(5\omega t) - \frac{\sqrt{3}}{2} cos(5\omega t)) \\ &= \sqrt{3} i_1 sin(\omega t + 30^\circ) - \sqrt{3} i_5 sin(5\omega t - 30^\circ) \end{aligned} \tag{11}$$

3.1.3 Even Harmonics

Even harmonics are defined as frequency components produced by non-linear loads with asymmetric I-U characteristics. These asymmetric non-linear loads can generate asymmetries in peak magnitudes of current and voltage waveforms and DC components. It can also generate asymmetries in the positive and negative half-period duration's and fluctuations in Root-Mean-Square (RMS) voltage [36]. In figure 2 the symmetry of the even harmonic wave is represented by the cosine wave, the blue line, as it is symmetric about the y-axis. Even harmonics are usually not measured in the electrical power system as they are negligibly small [9]. As they were not measured in Simris there neglected in this project.

3.1.4 Switched Waveforms

Diode bridges and power electronics have switching voltages. They are based on thyristors switching every network period and give harmonics that are integer multiples of the network frequency. Today, the dominating power electronics with transistors have a switching frequency of around 1-5 kHz and contribute to PWM-voltages. The easiest switching waveform is the rectangular wave. A Fourier analysis shows that it contains odd harmonics to the fundamental with the frequency fs [37]. Figure 5 below shows a rectangular wave and its harmonic spectrum.

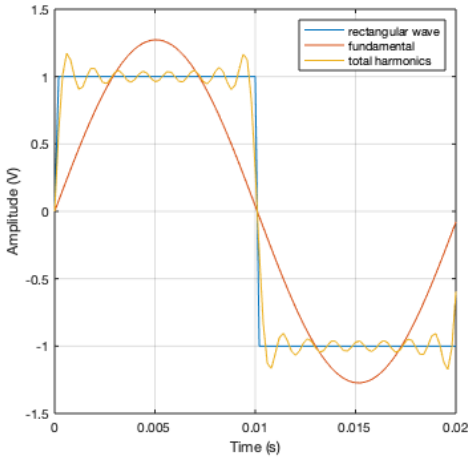

(a) Rectangular wave(blue), fundamental wave (orange) and the fundamental with added odd harmonics (yellow).

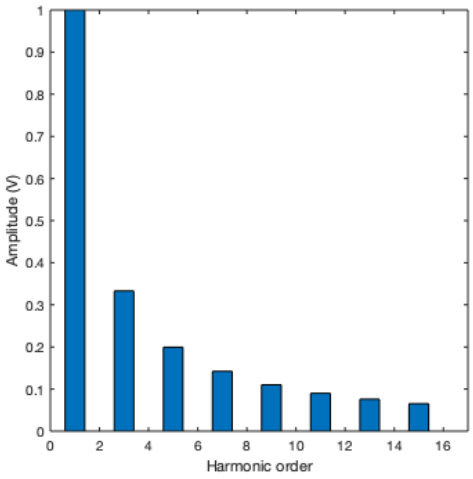

(b) Harmonic spectrum

Figure 5: The rectangular wave represented by the fundamental with added odd harmonics (left) and its harmonic spectrum (right).

3.1.5 Filtering Harmonics

The distortions caused by harmonic voltage can be eased by the application of passive or active power filters. Passive filters are less expensive to buy and operate, whilst active power filters can compensate harmonics in a wide range of frequencies [38]. A type of passive filters being used is shunt filters that are only rated for part of the voltage in the system, meaning that they required smaller components and are therefore cheaper. Shunt filters consist of three categories, single-tuned, multiple-tuned and damped, where single- and multiple tuned are generally used to filter specific frequencies. The damped filters, on the other hand, are used to filter a broader range of frequencies [39].

3.2 Power Quality Indices

Both individual harmonic content in a current or voltage waveform and all the harmonic content can be calculated as indices for harmonic distortion. The equation for calculating HD and total harmonic distortion (THD) will be presented in this subsection.

3.2.1 Relative Harmonic Distortion

Measuring HD is relative and involve measuring the effect of the harmonic on the fundamental. The formula to calculate individual harmonic voltage distortion is seen in equation 12 where V_n is the voltage of the n:th harmonic and V_n is the voltage of the fundamental. Individual harmonic current distortion is calculated similarly and is presented in 13 were I_n is the current of the n:th harmonic and I_n is the current of the fundamental [40].

$$HD_v = \frac{V_n}{V_1} \tag{12}$$

$$HD_i = \frac{I_n}{I_1} \tag{13}$$

3.2.2 Total Harmonic Distortion

THD is used to determine the level of harmonic content in voltage or current waveforms and can be defined in two different ways. In the first definition, the harmonic content of a waveform is compared to the voltage or current of the fundamental frequency and this definition is denoted THD_F. The THD_F equations for current, THD_{FI}, and voltage, THD_{FU}, are presented in equation 14 and 15 below, where I_n represents the RMS current of the n:th harmonic and U_n is the RMS voltage of the n:th harmonic. The first harmonic (n=1) is the fundamental frequency.

$$THD_{FI} = \frac{\sqrt{\sum_{n=2}^{\infty} I_n^2}}{I_1} \tag{14}$$

$$THD_{FU} = \frac{\sqrt{\sum_{n=2}^{\infty} U_n^2}}{U_1} \tag{15}$$

The second definition compares the harmonic content of a waveform to the waveforms RMS value and is denoted THD_R. The THD_R equations for current, THD_{RI}, and voltage, THD_{RU}, are presented equation 16 and 17 below [41].

$$THD_{RI} = \sqrt{\frac{\sum_{n=2}^{\infty} I_n^2}{\sum_{n=1}^{\infty} I_n^2}} \tag{16}$$

$$THD_{RU} = \sqrt{\frac{\sum_{n=2}^{\infty} U_n^2}{\sum_{n=1}^{\infty} U_n^2}} \tag{17}$$

THD_F can be seen as a measure of harmonic amplitude, whilst THD_R can be seen as a measure of how much of the total energy is in the harmonics. The relation between the two definitions can be shown in equation 18, where it can be seen that for low values there is not a significant difference between the two definitions [41]. At these values, the signal's spectrum is closer to the ideal one and there is less interference for other electronic equipment [42]. Whilst for high values the difference becomes important as THD_R cannot exceed 100%, however THD_F may reach higher values when the spectral energy of the harmonics surpasses the spectral energy of the fundamental frequency. The equation also shows that a large variation in THD_F appears as a small variation in THD_R and vice versa. Usage of THD_F is preferred as it is a considerably better measure of harmonic content [41].

$$THD_R = \frac{THD_F}{\sqrt{1 + THD_F^2}} \tag{18}$$

3.3 Guidelines for Voltage Harmonics

For a voltage reference, nominal voltage, less than or equal to 36 kV the following applies in Sweden [30]: During a period corresponding to a weeks time, the occurring ten-minute values for each individual HD should be less than or equal to the values in table 2. In addition, each ten-minute value of the total harmonic content should be less than or equal to eight percent.

Table 2: Limits for relative harmonic distortion for voltage references less than or equal to 36 kV according to the regulation EIFS 2013:1 [30].

Odd harmonics			
Not multiples of 3		Multiples of 3	
Harmonics (n)	Relative harmonic distortion	Harmonics (n)	Relative harmonic distortion
5	6.0 %	3	5.0 %
7	5.0 %	9	1.5 %
11	3.5 %	15	0.5 %
13	3.0 %	21	0.5 %
17	2.0 %		
19	1.5 %		
23	1.5 %		
25	1.5 %		

3.4 Harmonics in the Power Grid

The power grid influence on harmonic voltage and currents is discussed in this section.

3.4.1 Harmonic Load Flow

Harmonic load flow analysis is a way of quantifying voltage and current harmonics at different points in a power system to be able to avoid harmonic resonance and unwanted harmonic conditions [43]. A load flow model of a power system includes the network components harmonic characteristics. Figure 6 shows a circuit diagram of a simple network. The components are modelled according to recommended standards [44].

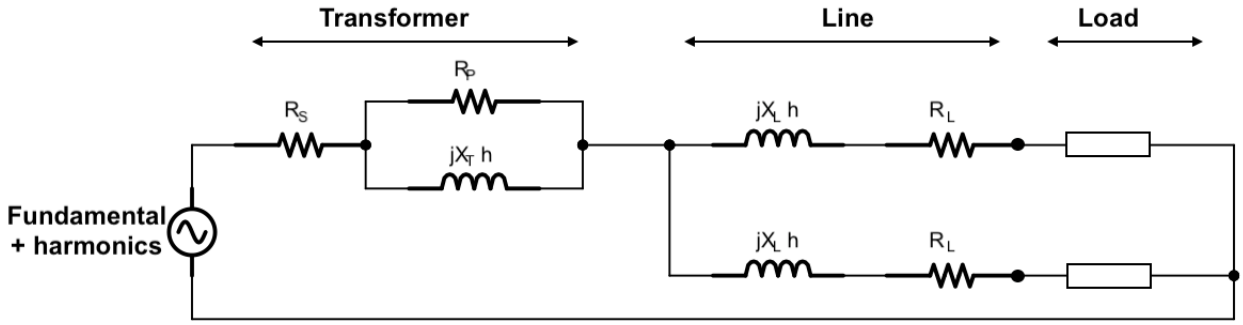

Figure 6: Circuit diagram with one phase of a power electronic source that is feeding two feeder lines and loads through a joint transformer.

Harmonic load flow analysis calculates voltages and currents for every harmonic at every point in the circuit. Series and parallel coupling work as usual and the impedance showed in the figure depends on the harmonic order. A high power system impedance and low fault current give a high harmonic voltage distortion [45]. The harmonic voltage levels in the power grid will affect the current harmonics through the grid impedance and vice versa [46].

3.4.2 Primary and Secondary Emissions

Primary harmonic emission is "the emission originating from the device" and secondary emission is "the emission originating outside the device" [47].

A simple explanation of harmonics is that a device injects current harmonics into the grid that appears as voltage harmonics in other parts of the grid. Devices with harmonic emissions are modelled as an ideal current source at the harmonic frequency independent of the voltage harmonics in the device connecting point. Unfortunately, harmonics are not that simple. The voltage harmonics in the grid connecting point of the device impacts the number of current harmonics. This makes the separation of the level primary and secondary harmonics more complex and hard to identify. Identifying the primary harmonics from a device connected to a power system might not be possible without controlled experiments or already knowing the harmonic spectra of the device [47].

3.4.3 Harmonic Resonances

Harmonic resonance occurs when the impedance in a circuit containing inductors and capacitors reaches a very high value - parallel resonance, or a very low value - series resonance. When parallel resonance occurs, there is an amplification of the harmonic currents and when series resonance occurs, there is an amplification of the harmonic voltage. A large amount of capacitance can also create resonance frequencies due to the long underground cables and capacitor banks [12].

3.5 Harmonic Emission Sources

Harmonic emissions can come from several different sources in a power grid. In this section harmonics from wind power, PV-plants and customer loads will be discussed.

3.5.1 Harmonic Emissions from Wind Power

Wind power impacts the power grid with harmonic levels through emissions and resonance frequencies that amplify the WT's emission. The severity of the impact is measured by calculating the percentage of the harmonic change related to the nominal current of the WT [12].

Harmonic emissions have become a more significant issue with the integration of modern WTs. When conventional energy generation is replaced with wind power, there is less short circuit capacity, which gives a weaker grid, raising the harmonic levels [12]. Harmonic emissions in the WT can come from strong variations in the power production's active power or fast changes that give a low-frequency disturbance [12]. A directly grid-connected induction generator in the WT can create harmonics relatively small compared to harmonics that modern turbines with electric power converters create. They create high-frequency harmonics on several kHz due to switching. Power transformers are also a source of harmonic emission during high RMS voltages [12].

Most common is the disturbance of low order harmonics where the 5th and 7th dominate [48]. From studies of multiple WTs of different kinds, the THD level remains the same independent of the power output. The same phenomenon is shown for individual harmonics except for a small harmonic and power correlation for the 5th order. The probability of the magnitude of a low order harmonic is distributed according to a normal distribution. [48].

3.5.2 Harmonic Emissions from PV-plants

Simris is provided with a photovoltaic (PV) system, which is an inverter-based type generator. The solar panel absorbs photons from the sun and a PV effect process creates electric direct current (DC). To be

able to connect the generator to the grid, an inverter is used to get alternating current (AC).

Inverter based equipment like a PV-plant will always inject current harmonics in the grid during generation. However, the harmonic level is not always connected to the amount of generation [49]. High levels of generation have shown to give low current harmonics levels in the percentage of the fundamental and the emissions are very low during little or no generation. The current harmonic emissions from PV-plants found in a study are similar to those for non-linear loads in LV grids. The most dominant harmonics are the low order odd current harmonic emissions. Some connection between fluctuation in the generation, phase angle and emission for a low generation has been shown [49].

3.5.3 Harmonic Emission from Customer Loads

It has been a change in the type of devices that are connected to the LV grid. More energy efficient devices like LED lamps are a great example of that. The use of switching transistors will not only allow energy efficient devices but do also distort the power grid with the switching frequency [49]. Non-linear loads that draw a non-sinusoidal current are also a reason for harmonics [50]. In table 3 the magnitude for individual current harmonics from customer loads is presented. The measurements were taken from a residential area in Sweden that was built in the 70's. The third harmonic is the biggest, which suggests that a lot of one phase rectifiers are used in the household equipment's [51].

Table 3: The average magnitude of individual current harmonics from a residential area built in the 70's, the measurements were taken i March 2013 [51].

Harmonic order	Magnitude
3	4.1%
5	2.6%
7	1.3%
9	1.6%
11	0.9%
13	0.6%
15	0.5%

4 Method

This section describes the overall method for answering each of the earlier formulated research questions. The points where data is collected and the model is validated are also presented.

The project workflow is presented in figure 7. The working method was first divided into two work parts, data analysis and modelling of the microgrid. The data analysis part consisted of analyzing a large amount of weather and collected microgrid data to answer the following research questions: *What is the relation between harmonics from renewable energy sources in the Simris microgrid and the weather?* and *How do electrical harmonics behave in grid-connected mode and island mode?* The modelling part refers to constructing a model of the Simris microgrid based on information about the actual grid and collected microgrid data. The model was then validated before simulations were conducted. Comparison between collected harmonic data and simulation results allowed us to answer the last research questions: *Is it possible to make a presentable model of Simris in the simulation program NEPLAN and what are the limitations of such simulations?*

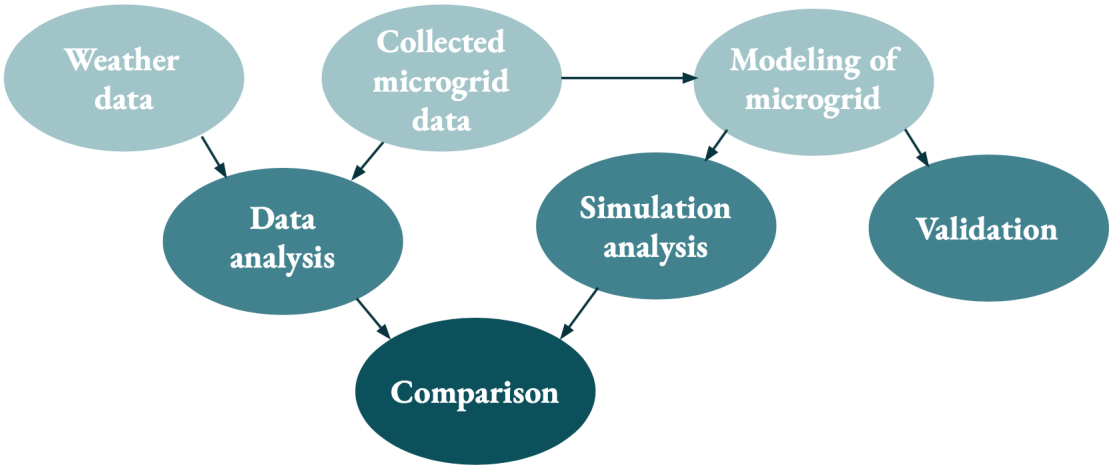

Figure 7: The project workflow.

Both data analysis and simulations were made for island mode and grid-connected mode. Island mode represents when the microgrid is not connected to the distribution grid, hence the X-GridPoint, in figure 8, is not connected to the microgrid. Grid-connected mode is when the microgrid is connected to the distribution grid, hence the X-GridPoint is connected to the rest of the microgrid.

The microgrid data was collected from three points, X-WT, X-PV and X-Load, which are seen as the navy blue points in figure 8. X-WT and X-PV were chosen to examine harmonics from wind and solar power and X-Load was selected to investigate the harmonic emissions that reach the connected customers. X-WT and X-Load are located on the LV side of the transformer and X-PV is located on the MV side of the transformer, affecting the values collected at these points. The validation was done in three nodes for island mode: X-PV, X-El_Joint2 and X-Load. X-PV was chosen to see if the model is valid at one of the harmonic sources, X-El_Joint2 was chosen to see if and how the BUG and Li-Battery affect the load flow and lastly, X-Load was selected to see if the model was valid at a consumer node. For grid-connected mode, the validation was made at the previously mentioned points and X-GridPoint to see if and how the distribution grid affects the validation. All the validation points are marked in green in figure 8.

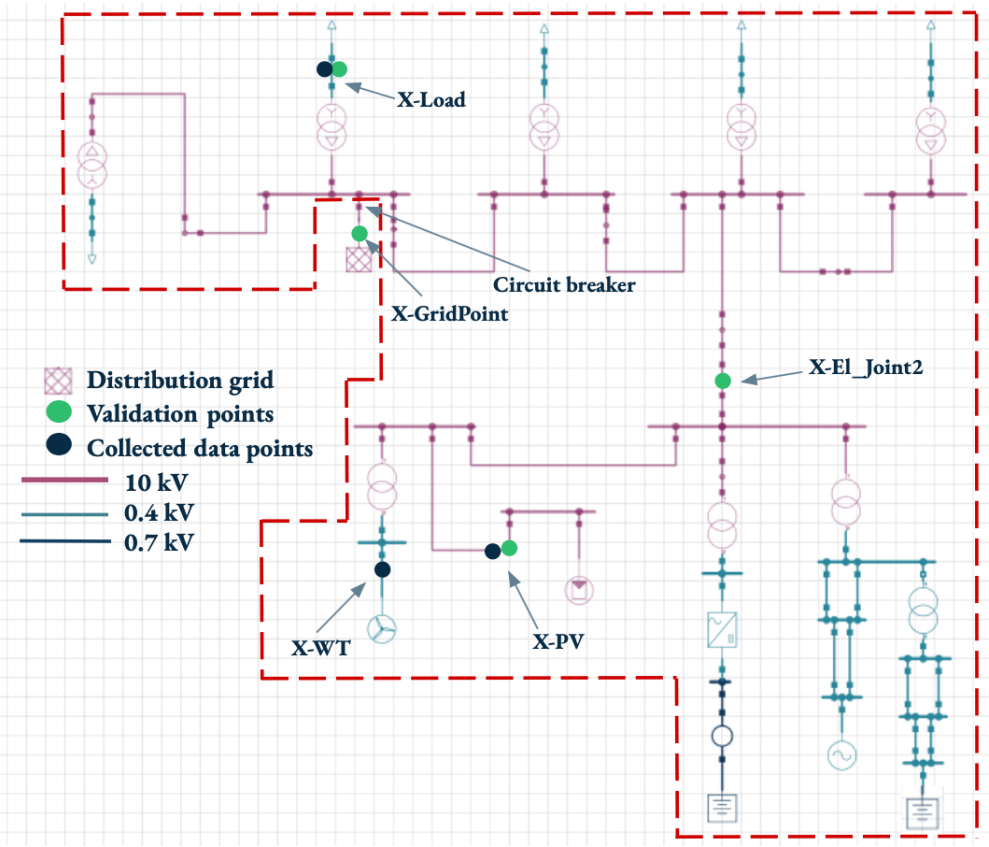

Figure 8: The placement and names of the collected data points(navy blue) and validation points(green). The checked box represents the distribution grid and the red marked area is the grid in island mode.

5 On-site Collected Data

In this section collected harmonic data is analysed at three different points in the microgrid during island mode and grid-connected mode. The harmonic emissions from wind power generation and solar power generation are put in relation to local weather measurements. The harmonic content is also investigated at a load point in the microgrid.

5.1 Collected Data Management

Large amounts of local weather data were compared to the collected microgrid data at three different points in the microgrid. Microsoft Excel was used to analyse individual harmonics and THD during island mode and grid-connected mode. The harmonic levels were then compared to voltage harmonic guidelines.

5.1.1 Weather Data

The weather data used in the project is taken from SMHI weather station in Skillinge, 4.5 km away from the WT and the PV plant in Simris. From the weather data, days with different weather conditions were selected for further investigation. The days with different combinations of wind speed and irradiation were used to study the correlation between weather and harmonic emissions. The effect of solar irradiation and wind speed levels were studied when the microgrid was both grid-connected and run in island mode.

5.1.2 Microgrid Data

Measurements at different points in the microgrid were collected during the Simris LES project(2017-2021). The time periods chosen for analysis of collected data were dependent on access to information about when the system was in island mode and grid-connected mode. Additionally, the selected days with different weather condition determined the dates and times that were chosen for analysis. In grid-connected mode, a minimum of two hours during five days in January, July and October was chosen for analysis while for island mode collected data from three days in November were analysed.

X-WT, X-PV and X-Load, see section 4 for more details, are the collecting points for the data that were analysed in this thesis. X-WT is located on the LV side of the transformer and is chosen to analyse harmonics generated by the wind turbine. X-PV is located on the MV side of the transformer and is chosen to analyse harmonics from the PV plant. The last point, X-Load is located on the LV side of the transformer where customers, also called loads, are connected and is the point chosen to investigate the power quality that reaches the end customer. Data collection was achieved using different types of data analysers. These systems are built on different analysis standards, but the difference was considered negligible for this project, see section 2.2.4 for more details.

Current individual harmonics and THD were analysed in X-PV and X-WT, while voltage individual harmonics and THD were analysed in X-Load. This has to do with how primary and secondary emissions appear in the grid and is explained in section 3.4.2. The data consist of 10-minute values for THD and odd individual harmonics from 1st-15th harmonic. All the data were analysed for just one of the three phases.

The harmonic emissions in the three different collecting points are analysed below. All plots from X-WT are blue or purple, while plots from X-PV are orange or red and finally, plots from X-Load are green.

5.2 Collected Data Analysis at X-WT

Figure 9 shows the correlation between the measured wind speed and the fundamental current of the wind turbine. At low wind speeds, see figure 9a, the slope is positive and the fundamental current is increasing with the wind speed. Figure 9b is the current during high wind speeds, which is almost consistent at 690 A. This is because the WT reaches its maximum power at 12m/s and the fundamental is constant above that point. The correlation between the wind speed and the fundamental current is the same for when the system is connected to the distribution grid and when it is in island mode.

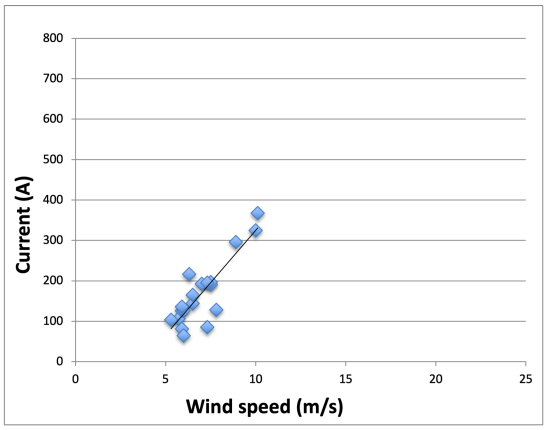

(a) Light winds (5-12 m/s)

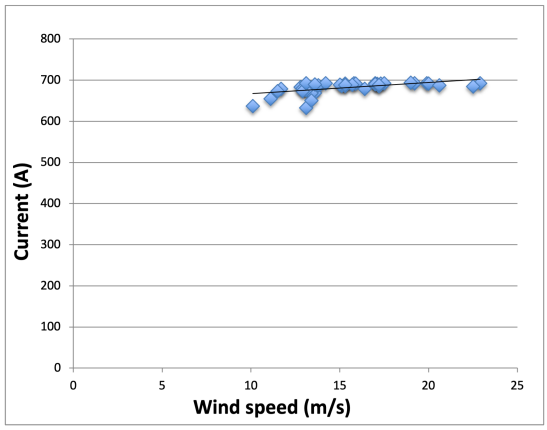

(b) Strong winds (above 12 m/s)

Figure 9: The fundamental current in relation to wind speed, in grid-connected mode for light and strong winds. Data collected: (a)October 15th 09:00-12:00 and (b)January 1st 00:00-07:00.

In figure 10 the fundamental current is shown for wind speeds just around the WT cut-in point. There are multiple points below the cut-in at 2,5 m/s that produce around 20 A, which theoretically should not be possible, but there is a distance of 4.5 km between the WT and the weather station, resulting in a time delay. This time delay is considered a source of error between the weather data and collected data. The wind turbine also stores energy in the rotor blades, so the turbine does not turn off immediately when the wind drops below 2,5 m/s.

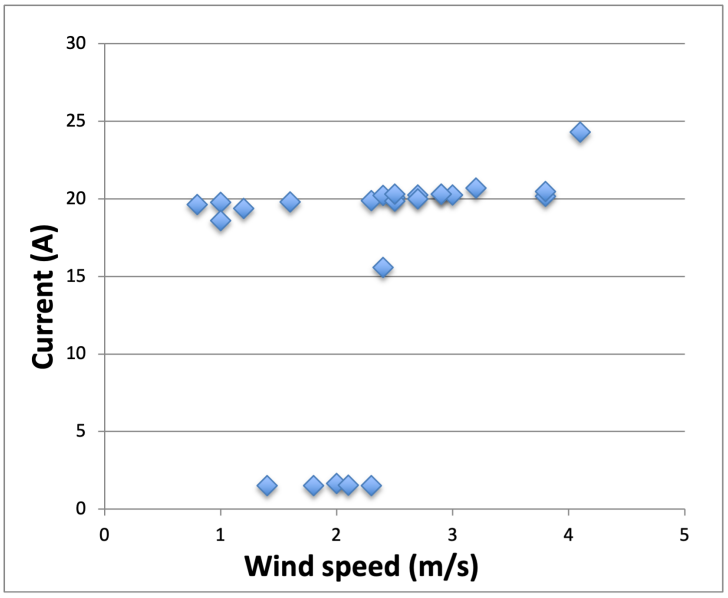

Figure 10: The fundamental current around the WT cut off point at 2.5 m/s in grid-connected mode. Data collected: July 1st 00:00-04:00.

Figure 11 shows the harmonic content in X-WT during grid-connected mode when both the WT and the PV-panels are not in operation. There are low levels of individual current harmonics, but the voltage THD is 1.7%. This means a relatively high level of harmonic emissions in the grid not originating from wind power and solar power generation.

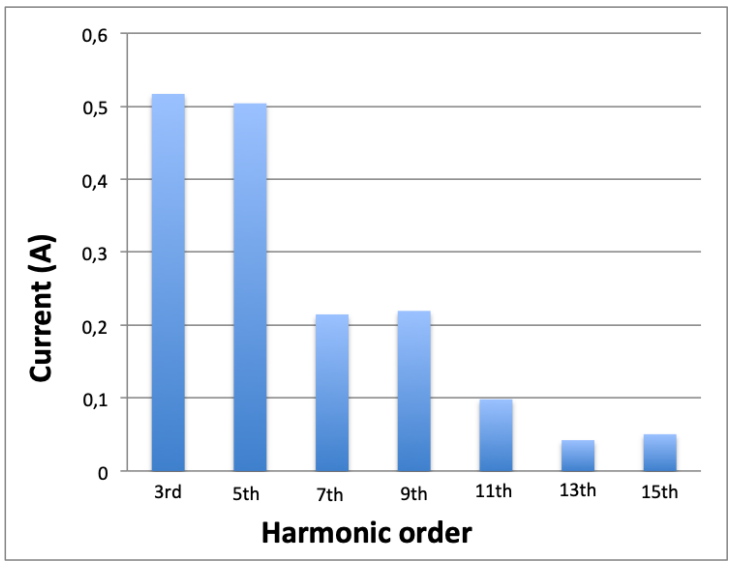

Figure 11: The individual harmonics content in X-WT when the WT and PV Park is shut off due to no wind or irradiation. Data collected: July 1st 01:00.

5.2.1 Current harmonics during low wind speeds

At wind speeds below 12 m/s the wind turbine production is changing with the wind speed as in figure 9a above. This also means that the wind measurement errors may be more evident because of the fast changes in the wind speed. The individual harmonics for light winds during grid-connected mode are showed in figure 12 - 15. There is not a clear connection between the wind speed and the current harmonics overall but the 5th, 7th, 11th and 13th harmonics have more scattered points which seems to have a slight increase with the wind speed. The same pattern is shown when the system is in grid-connected mode and island mode.

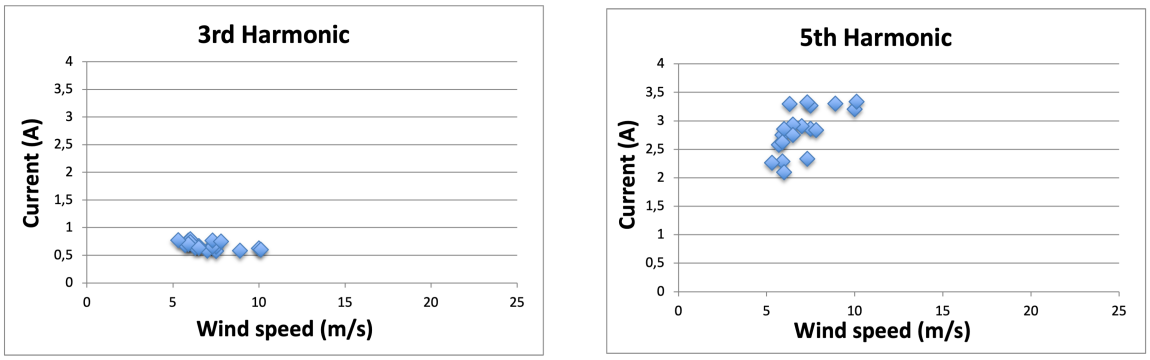

Figure 12: 3rd and 5th current harmonic for low wind speeds and grid-connected mode. Results for island mode are similar. Data collected: October 15th 09:00-12:00.

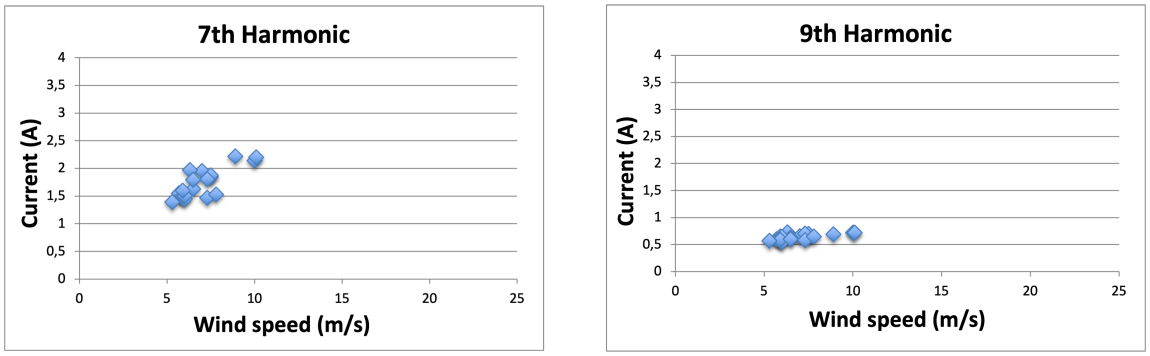

Figure 13: 7th and 9th current harmonic for low wind speeds and grid-connected mode. Results for island mode are similar. Data collected: October 15th 09:00-12:00.

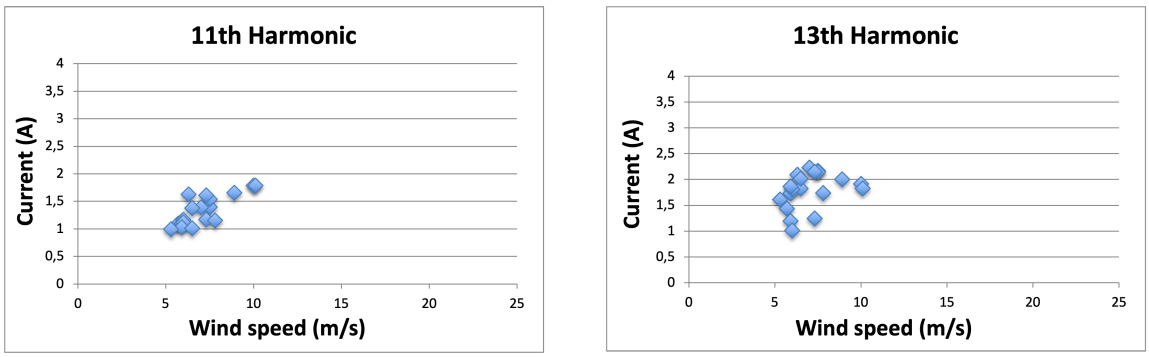

Figure 14: 11th and 13th current harmonic for low wind speeds and grid-connected mode. Results for island mode are similar. Data collected: October 15th 09:00-12:00.

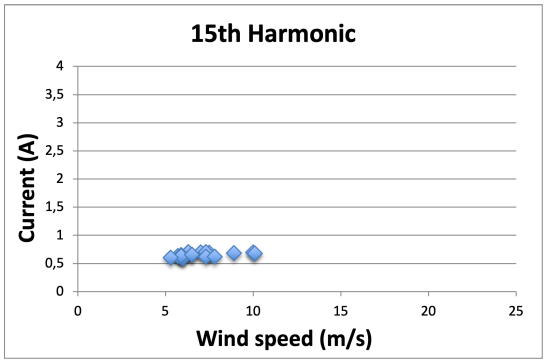

Figure 15: 15th current harmonic for low wind speeds and grid-connected mode. Results for island mode are similar. Data collected: October 15th 09:00-12:00.

To see the severity of the harmonics, the individual harmonics content is measured as a percentage of the rated fundamental current. Figure 16 shows the individual harmonics currents in percentage for when the system is in grid-connected and island mode. The 5th harmonic appears to be the largest one while the 3rd, 9th and 15th are the smallest.

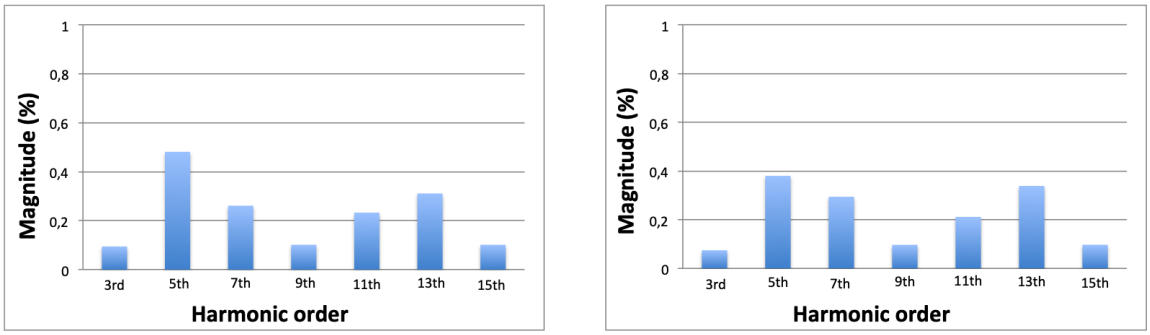

(a) Grid-connected mode **(b)** Island mode

Figure 16: Individual harmonics content in percentage of rated current for wind speed 7,3 m/s in figure a and 8,7 m/s in figure b. Data collected: (a)October 15th 10:10 and (b)November 10th 18:50.

The current THD is misleading during very light winds. The harmonic levels seen in figures 12 - 15 are compared against a low fundamental current during lighter winds and give current THD on 5-20 %. The voltage THD in the X-WT is shown in figure 17. The voltage THD levels are a little higher during grid-connected mode than during island mode. If voltage THD levels when there is no wind or solar generation at 1.7 % are compared with the levels when there is generation as in 17a, it can be seen that the majority of the THD content probably appears from somewhere else in the grid.

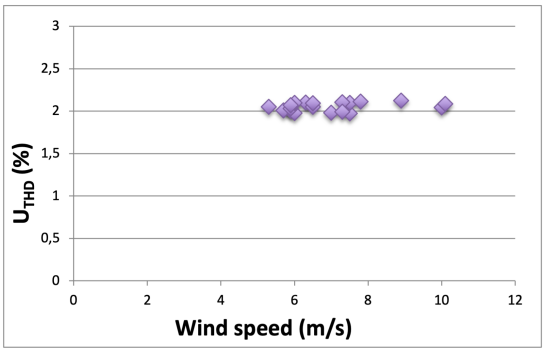

(a) Grid-connected mode

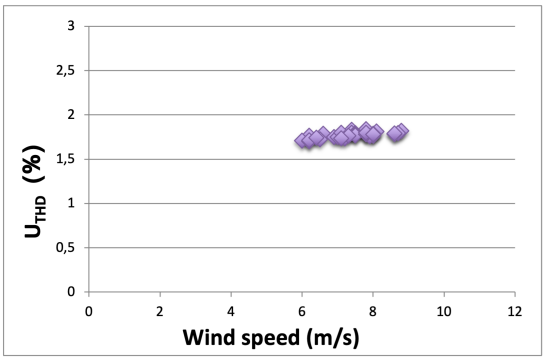

(b) Island mode

Figure 17: Voltage THD during light winds. Data collected: (a)October 15th 09:00-12:00 and (b)November 10th 17:00-22:00.

5.2.2 Current harmonics during high wind speeds

The wind turbine reaches its rated power at 12m/s, meaning that production at wind speeds above 12 m/s can be seen as constant. For these high wind speeds, the individual harmonics are also close to constant. Figure 18-21 shows the individual current harmonics for higher winds in grid-connected mode. These strong winds were not found in the data for island mode and therefore are the figures shown below in this section measurements during the grid-connected mode. The current harmonic levels are similar to the levels for wind speeds below 12 m/s and the 5th and 7th harmonic order are the largest ones in both cases. This confirms that there is a small correlation between the individual current harmonics and the wind speed.

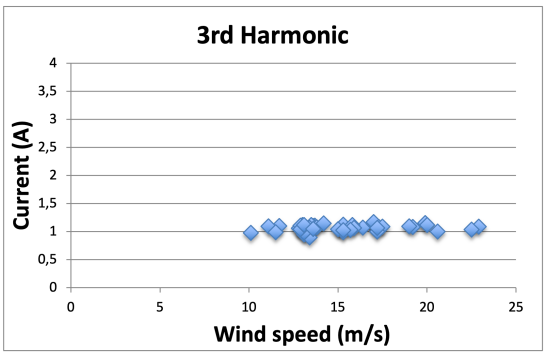

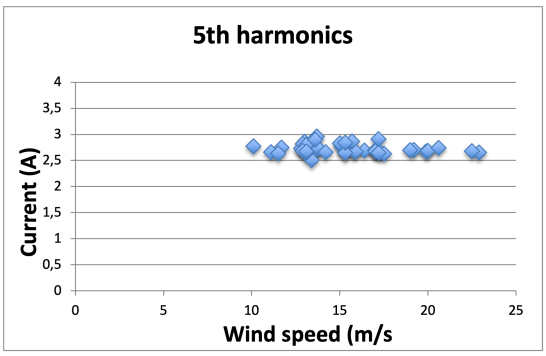

Figure 18: 3rd and 5th current harmonic for high wind speeds and grid-connected mode. Data collected: January 1st 00:00-07:00.

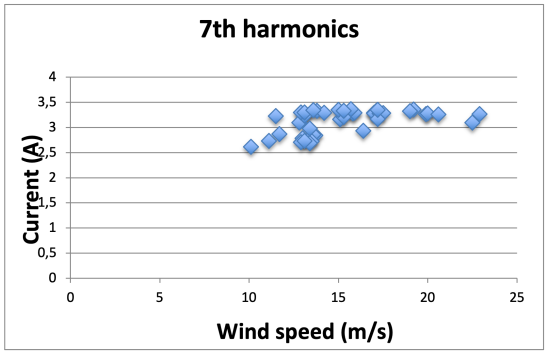

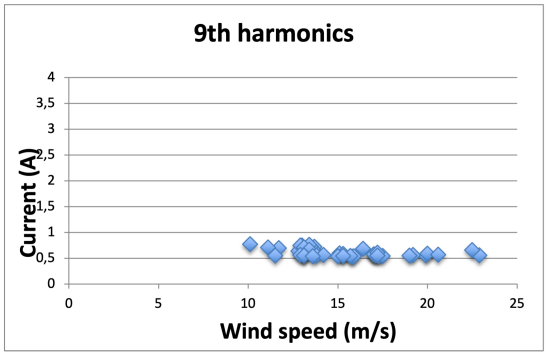

Figure 19: 7th and 9th current harmonic for high wind speeds and grid-connected mode. Data collected: January 1st 00:00-07:00.

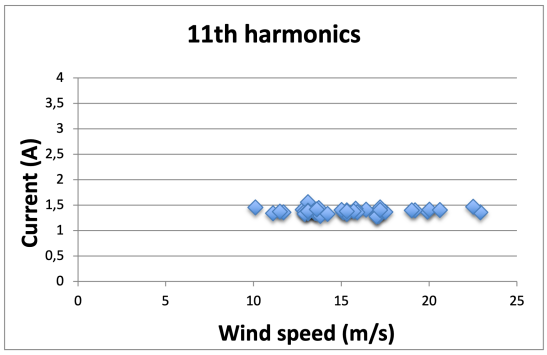

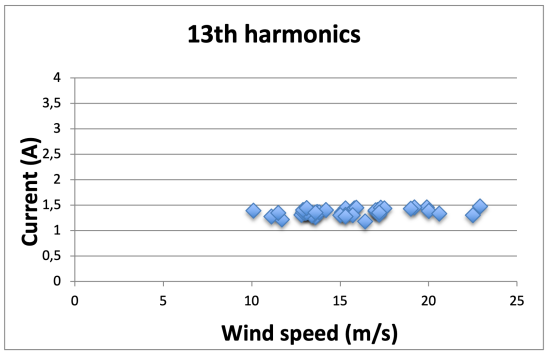

Figure 20: 11th and 13th current harmonic for high wind speeds and grid-connected mode. Data collected: January 1st 00:00-07:00.

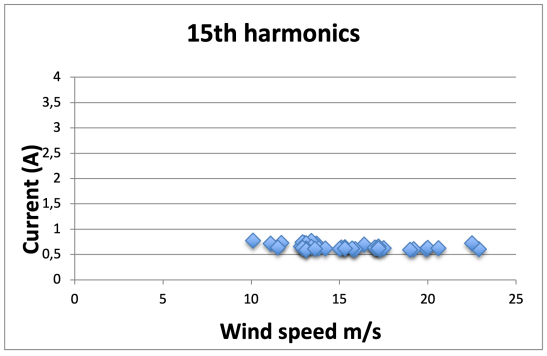

Figure 21: 15th current harmonic for high wind speeds and grid-connected mode. Data collected: January 1st 00:00-07:00.

Figure 22 shows the individual current harmonics contents as a percentage of the rated fundamental current for strong winds during the grid-connected mode. In this case, the 5th and 7th harmonic orders are the largest.

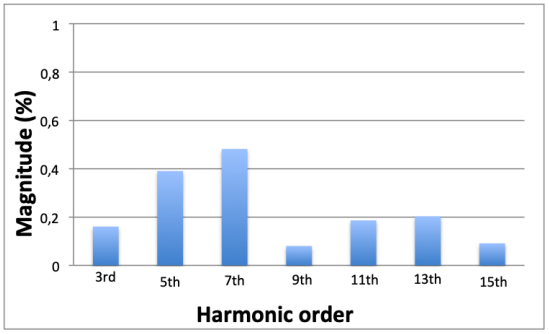

Figure 22: Individual current harmonic content during wind speed 17,1 m/s for grid-connected mode. Data collected: January 1st 03:10.

Figure 23 shows the voltage THD level for wind speeds above 12 m/s when the system is connected to the distribution grid. The current THD is 1.7 % at high wind speeds.

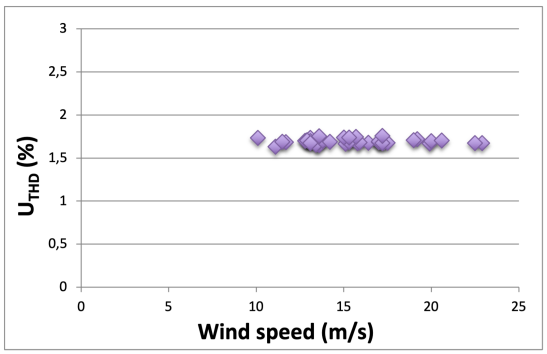

Figure 23: Voltage THD during strong wind speeds when the system is in grid-connected mode. Data collected: January 1st 00:00-07:00.

5.3 Collected Data Analysis at X-PV

The correlation between the irradiation and the fundamental current is y=0,02x, where y is the current and x is the irradiation. Figure 24 shows the irradiation and fundamental current for a sunny summer day. During a cloudy day, the irradiation changes fast during the day, but the same correlation is found between irradiation and the fundamental current. Fast changes in irradiation give some scattered points that might be an effect of the time delay between the met mast and the PV-installation or the clouds.

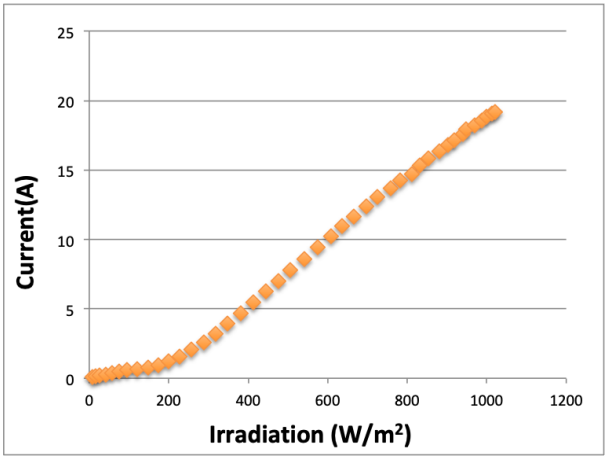

Figure 24: The measured irradiation and the fundamental current from early morning to noon in grid-connected mode. Data collected: July 20 05:00-12:00

When there is no irradiation, the current harmonics are close to zero in X-PV. The voltage THD is, on the other hand, 1.2-1.8 % both when the system is in grid-connected and island mode. The emissions appearing in the collected data are originating from other parts of the grid, like the WT, distribution grid, inverters and connected customers.

5.3.1 Current individual harmonics

Figure 25- 28 shows the individual current harmonic content when the system is in grid-connected mode. The 5th harmonic increases with the irradiation, which is just seen for grid-connected mode and not for island mode. This connection between irradiation and the 5th harmonic is not found in other studies. Why the same effect is not shown in island mode is unclear because the PV-installation primary emission should be the same independent of grid-connected or island mode. Nevertheless, voltage harmonics can affect the current harmonics through the grid impedance, which can change when the system is in island mode compared to grid-connected mode.

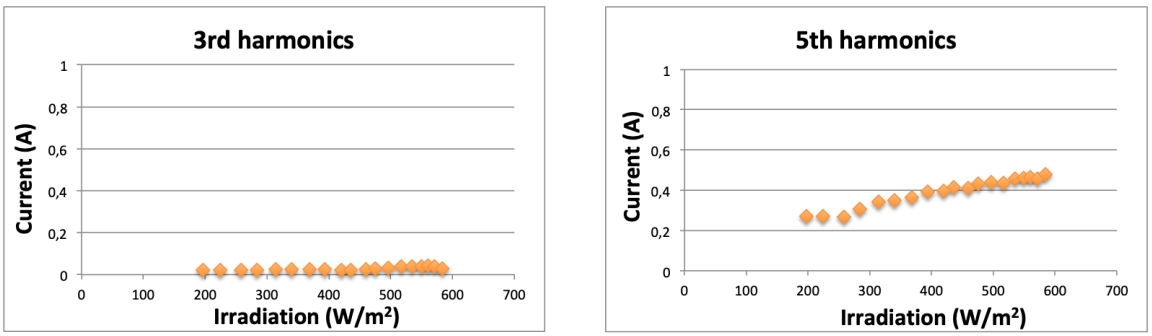

Figure 25: 3rd and 5th current harmonic content in grid-connected mode. Data collected: October 15th 09:00-12:00

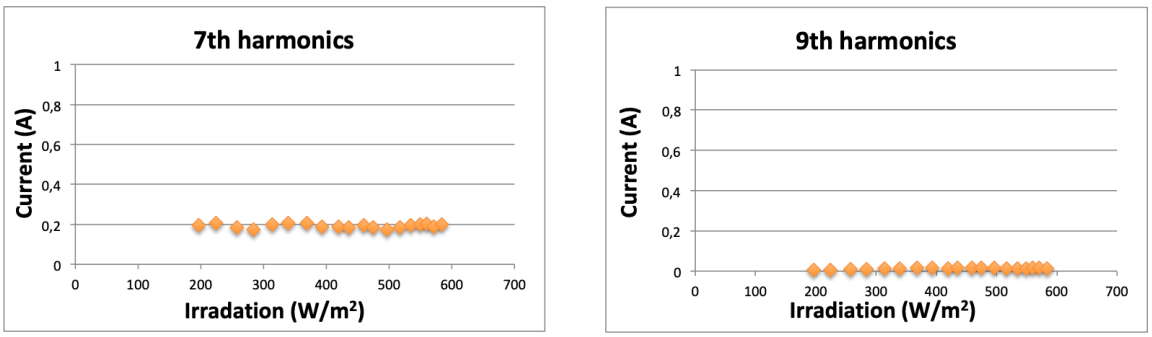

Figure 26: 7th and 9th current harmonic content in grid-connected mode. Data collected: October 15th 09:00-12:00

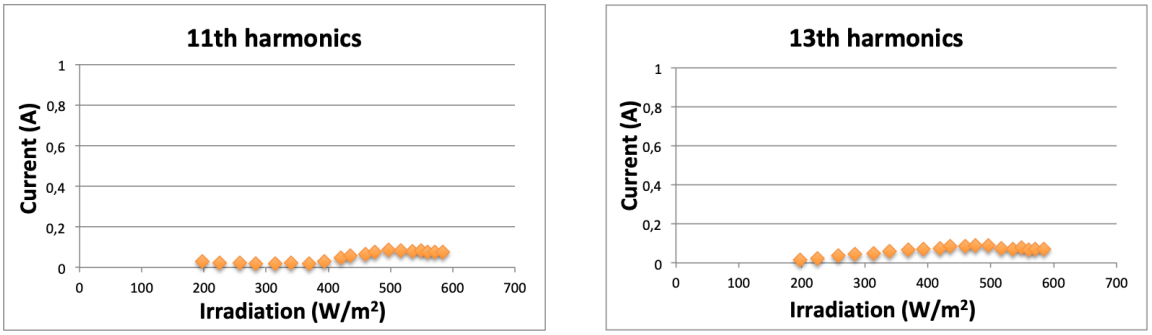

Figure 27: 11th and 13th current harmonic content in grid-connected mode. Data collected: October 15th 09:00-12:00

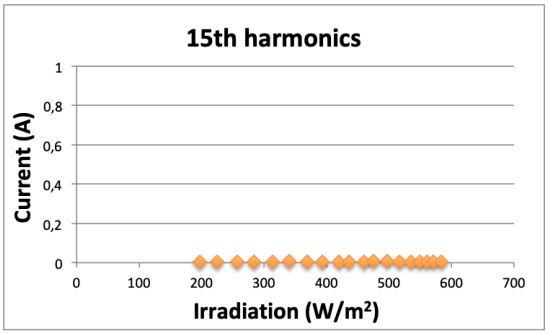

Figure 28: 15th current harmonic content in grid-connected mode. Data collected: October 15th 09:00-12:00

Figure 29 shows the current harmonic levels for the different orders when the system is in grid-connected and island mode. The 5th and 7th harmonics are the largest ones in both cases, but they are slightly smaller in island mode. The transformer between the LV grid where the PV installation is connected and the MV grid where the collecting point is located, should in a perfectly balanced system, block the 3rd, 9th and 15th harmonics. The theory behind this is explained in section 3.1.1. The 3rd, 9th and 15th order in figure 29 show low harmonic levels, which indicates that the system is not perfectly balanced.

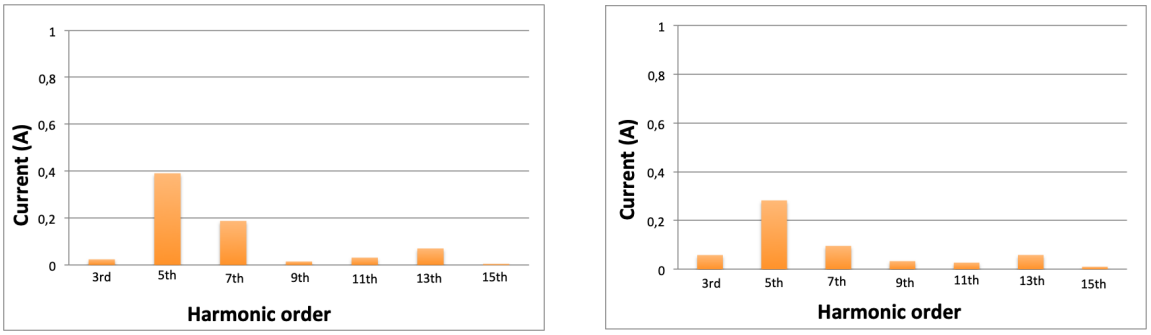

(a) Grid-connected mode

(b) Island mode

Figure 29: The individual current harmonic levels in X-PV. Data collected: (a)October 15th 10:10 and (b) November 7th 12:00

5.3.2 Current and Voltage THD

The current THD is a relationship between all the individual current harmonics and the fundamental current. For very low irradiation, a division of something close to zero is done and therefore gives a very high current THD as seen in figure 30. The current harmonic levels are below 1 A but appear very big when the fundamental is small, so this value gives an unfair image of the current harmonics during low irradiation.

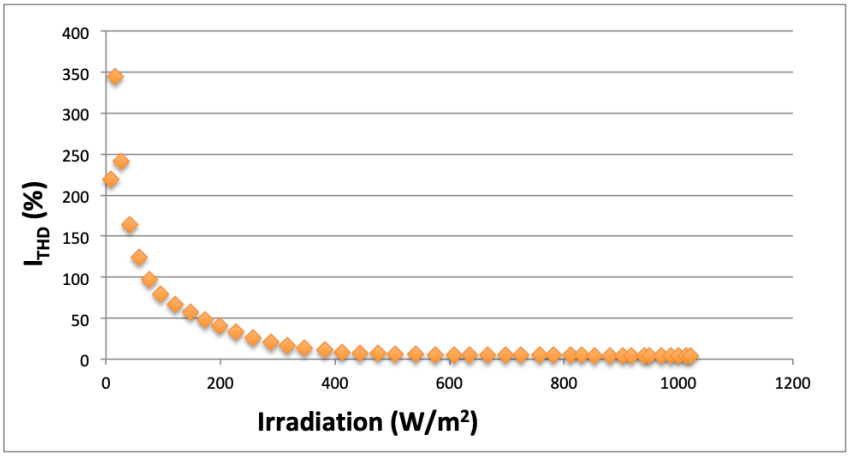

Figure 30: Current THD in grid-connected mode. Data collected: July 20 05:00-12:00.

Figure 31 shows the voltage THD when the system is in grid-connected and island mode. The harmonic level is higher in figure 31a than figure 31b most likely due to emissions originating from the distribution grid or other components in the microgrid.

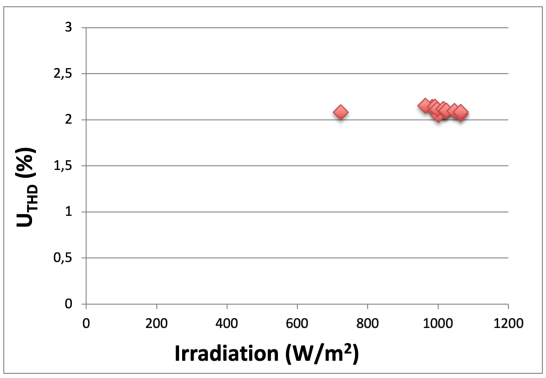

(a) Grid-connected mode

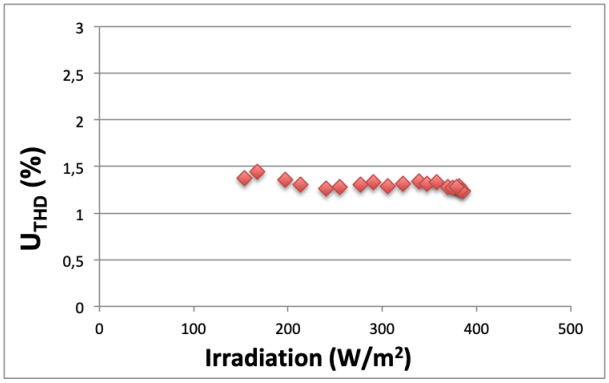

(b) Island mode

Figure 31: Voltage THD. Data collected: (a)July 8th 10:00-12:00 and (b)November 7th 10:00-12:00

In one specific case, the voltage THD has a "wave" shape shown in figure 32. The same shape is found in the current harmonics 5th and 7th order, see figure 33. Current harmonics influence voltage harmonics and vice versa and it is not always easy to know where the harmonic is originating from. However, this shape is not shown frequently in the collected values, making it more evident that it is a harmonic originating from somewhere else in the grid. The same phenomenon is found in island mode between voltage THD and the 5th harmonic current, see figure 34.

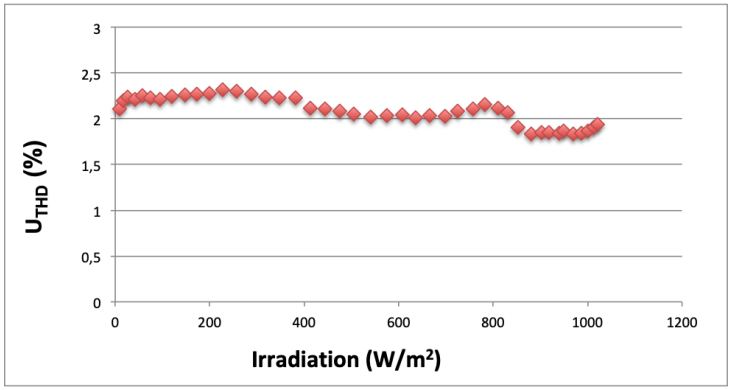

Figure 32: Voltage THD at X-PV during grid-connected mode. Data collected: July 20 05:00-12:00.

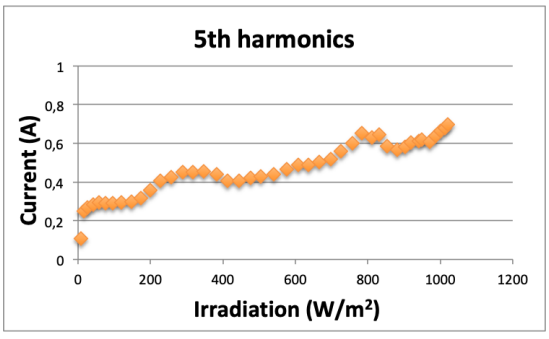

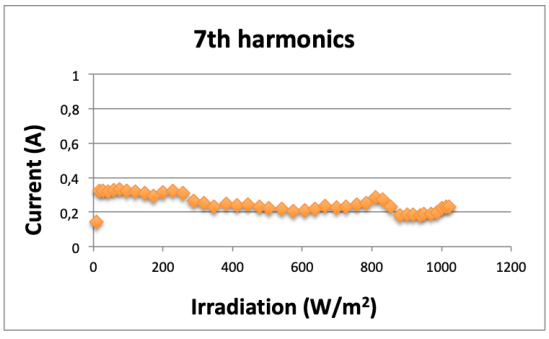

Figure 33: The individual current harmonic levels for the 5th and 7th harmonic during grid-connected mode. Data collected: July 20 05:00-12:00.

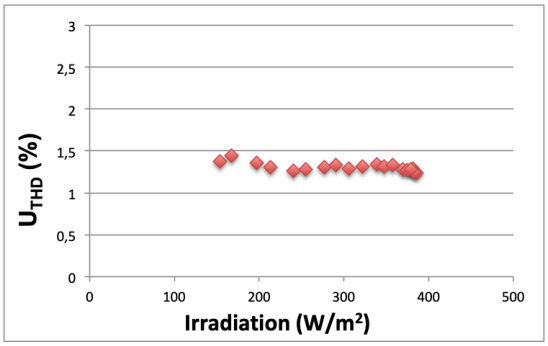

(a) Voltage THD

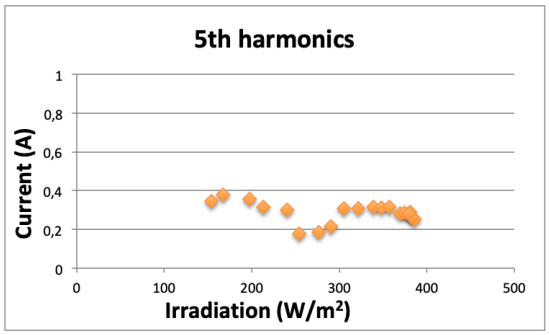

(b) Individual harmonic of the 5th order

Figure 34: Voltage THD (red) and the 5th harmonic current (orange) in X-PV during island mode. Notice that the left figure is voltage and the right figure is current and therefor the axis scaling is different. Around 250 $W/m2$ there is a voltage dip and around the same time there is a current dip. Data collected: November 7th 09:00-12:00.

5.4 Collected Data Analysis at X-Load

Figure 35 shows the individual voltage harmonics in X-Load when the system is in grid-connected mode. The 5th and 7th harmonic are the largest ones. Two different patterns in the figures where found: one when the PV-panels were producing and the other when they were not producing energy. When there was no PV production, see figure 35a, the 7th harmonic was the largest one but when there was production, see figure 35b, the 7th harmonic stayed on the same level and the 5th harmonic increased and became the largest one. The same effect can be seen when the system is in island mode but then the 5th and 7th harmonic levels are smaller in magnitude, see figure 36. It should be considered that the harmonics shown in this node are originating from the WT, PV Park, distribution grid, inverters and loads connected to the microgrid. The triplen harmonic levels are probably due to emissions from the connecting customers and unbalance in the network. Nevertheless, the harmonics shown in the X-PV are very similar to the one seen in the X-Load when the PV-panels are producing power.

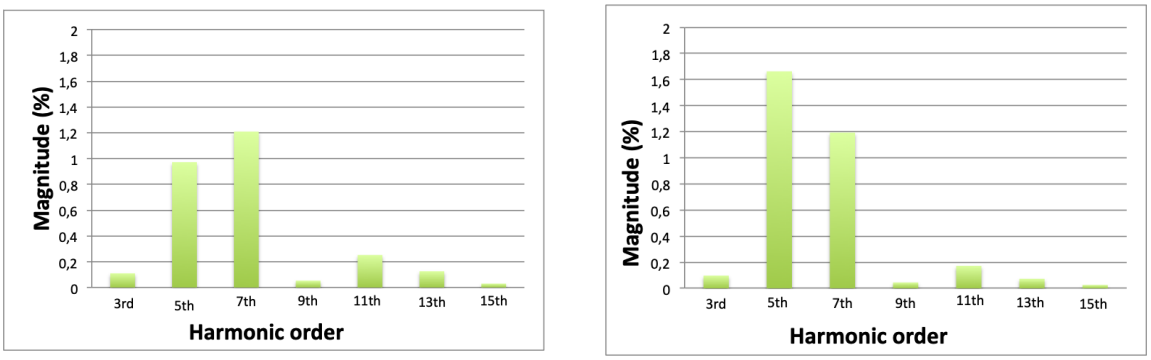

(a) No PV production

(b) PV production

Figure 35: Voltage harmonics as a percentage of the fundamental in the X-Load during grid-connected mode. Data collected: (a)July 1st 01:00 and (b)July 8th 11:10.

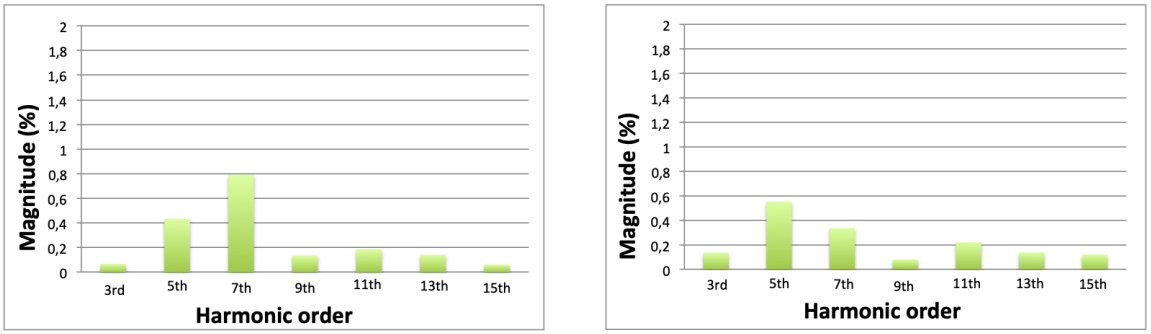

(a) No PV production

(b) PV production

Figure 36: Voltage harmonics as a percentage of the fundamental in X-Load during island mode. Data collected: (a)November 6th 22:10 and (b)November 7th 10:10.

The voltage THD in X-Load is similar to the THD in both X-WT and X-PV. Figure 37 shows the voltage THD against the wind speed in X-Load and X-WT. Both collecting points are located on the LV side of the transformer. The points are very similar, but the THD is about 0.5 % lower in the load point. Figure 38 shows the same voltage THD plotted against irradiation in X-Load and X-PV. Figure 38a and 38b are almost identical in shape and size, which shows that the harmonic content seen in the MV grid

is what is seen at the LV side at X-Load.

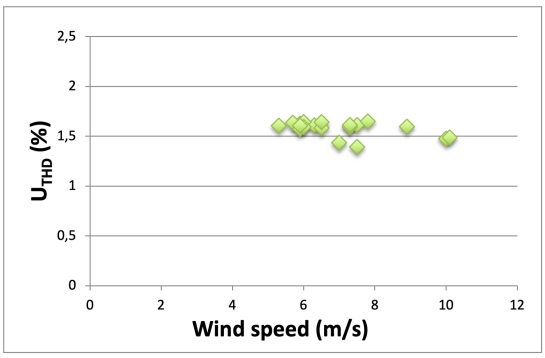

(a) X-Load

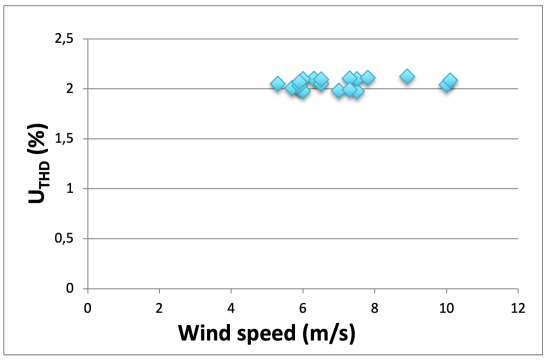

(b) X-WT

Figure 37: Voltage THD against wind speed at the same moment in time when the system is in grid-connected mode. Data collected: November 15th 09:00-12:00.

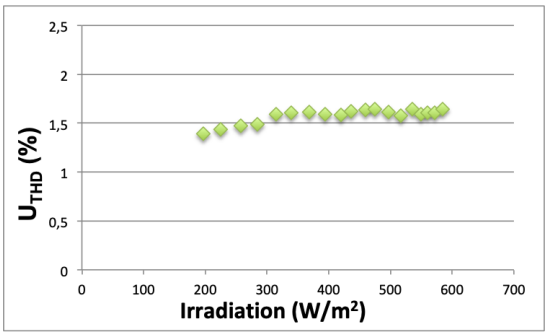

(a) X-Load

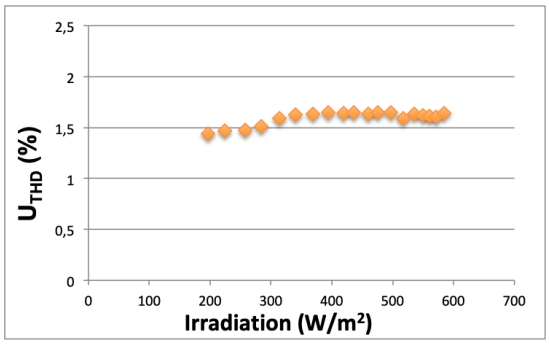

(b) X-PV

Figure 38: Voltage THD and the irradiation at the same moment in time when the system is in grid-connected mode. Data collected: November 15th 09:00-12:00.

The same observations have been seen when the system is in island mode. Figure 39 shows the voltage THD against wind speed in X-Load and X-WT, where the levels in the two plots differ by 0.7 %. Figure 40 shows the voltage THD against irradiation in the two collecting points during island mode.

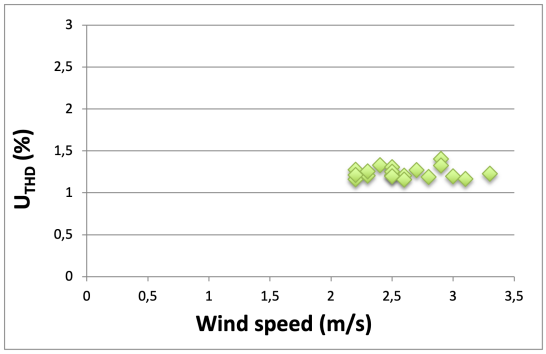

(a) X-Load

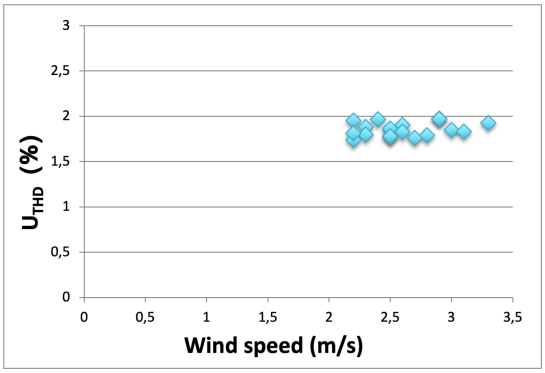

(b) X-WT

Figure 39: Voltage THD and the wind speed at the same moment in time when the system is in island mode. Data collected: November 7th 09:00-12:00.

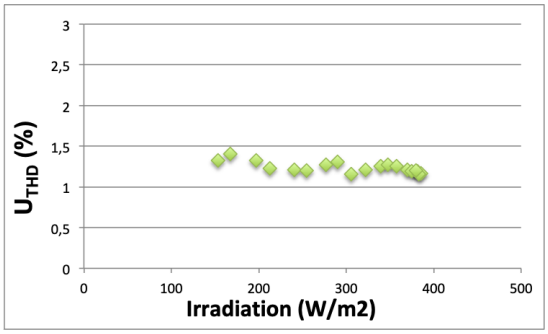

(a) X-Load

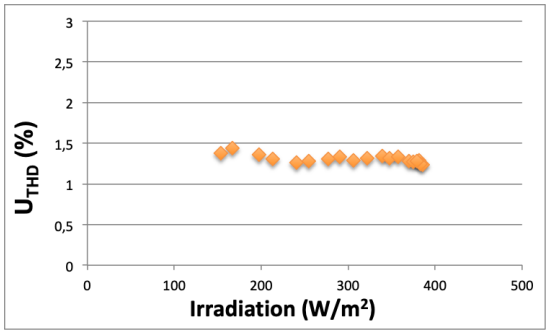

(b) X-PV

Figure 40: Voltage THD and the irradiation at the same moment in time when the system is in island mode. Data collected: November 7th 09:00-12:00.

5.4.1 Voltage harmonic requirements

Table 4 concludes the largest voltage harmonic values found in the data studied at X-Load and put them in comparison with the EIFS 2013:1 regulations. More information about the regulations can be read in section 3.3. The on-site collected harmonics at grid-connected and island mode are far below the requirements.

5.5 Conclusions from Collected Data Analysis

Harmonic distortion from renewable energy
In the on-site collected data, no clear connection between the weather and the harmonic levels could be found, with an exception for the 5th harmonic in X-PV. The harmonic emissions are almost on a constant level independent of the amount of production as long as the source is in operation. Out of operation, on the other hand, gives harmonic emissions close to zero. This effect is documented several times for both WT and PV plants. The voltage harmonics and THD were within the requirements at all times when the system was studied.

Harmonic level in the grid

Table 4: Voltage harmonics at X-Load in relation to the EIFS 2013:1 regulations.

	Grid-connected mode	island mode	Voltage harmonic regulations [30]
VTHD (%)	2.17	2.11	8
3rd (%)	0.18	0.42	5
5th (%)	1.88	1.06	6
7th (%)	1.30	0.92	5
9th (%)	0.08	0.21	1.5
11th (%)	0.36	0.37	3.5
13th (%)	0.15	0.18	3
15th (%)	0.09	0.13	0.5

The harmonic emissions seen in the microgrid are not only due to WT and PV generation. The customers connected to the grid could be considered both as load and generator, which are both a source of harmonic emissions. There are also harmonic emissions coming from the distribution grid when the system is in grid-connected mode. The voltage harmonic emission was between 1.2-1.8 % when the PV and WT generations were turned off, which means that there have to be other sources for harmonic emission that affect the harmonic level in the grid equally as much as the renewable generation. In a perfectly balanced system, the transformers would block the 3rd, 9th, and 15th harmonics and very low levels of those harmonics were seen in the MV grid compared to the LV grid. Low order harmonics like the 5th and 7th order spread very far in the grid.

Grid-connected vs. island mode
As discussed above, some harmonic emission comes from the distribution grid and influences the microgrid's harmonic levels when the system is in grid-connected mode. This is probably why higher THD levels can be seen when the system is in grid-connected mode and lower levels during island mode. A change in the grid impedance does also affect the harmonic levels.

Errors
There are some things to keep in mind when looking at the analysed data. The weather station is located 4.5 km from the WT and the PV installation, giving a time delay in certain collected data, especially when there are fast weather changes. The different collecting points are located on different sides of the transformers. The harmonics should be larger on the LV side of the transformer where the generation is located as transformers block triplen harmonics, as discussed in section 3.1.1. Only one of the phases and its 10-minute value was studied during a limited amount of time. These are all sources of error.

6 Modelling and Simulations

This section goes through the modelling process of the Simris microgrid in NEPLAN, the simulation program. A validation of the model and the simulation results in comparison to the collected data are also presented in this section.

6.1 Modelling

The model of the microgrid was made in the simulation program NEPLAN. The simulation software used was requested by E.ON and the model is based on an electrical line diagram provided by E.ON. Figure 41 shows the model where all the loads, energy sources, batteries and nodes are included.

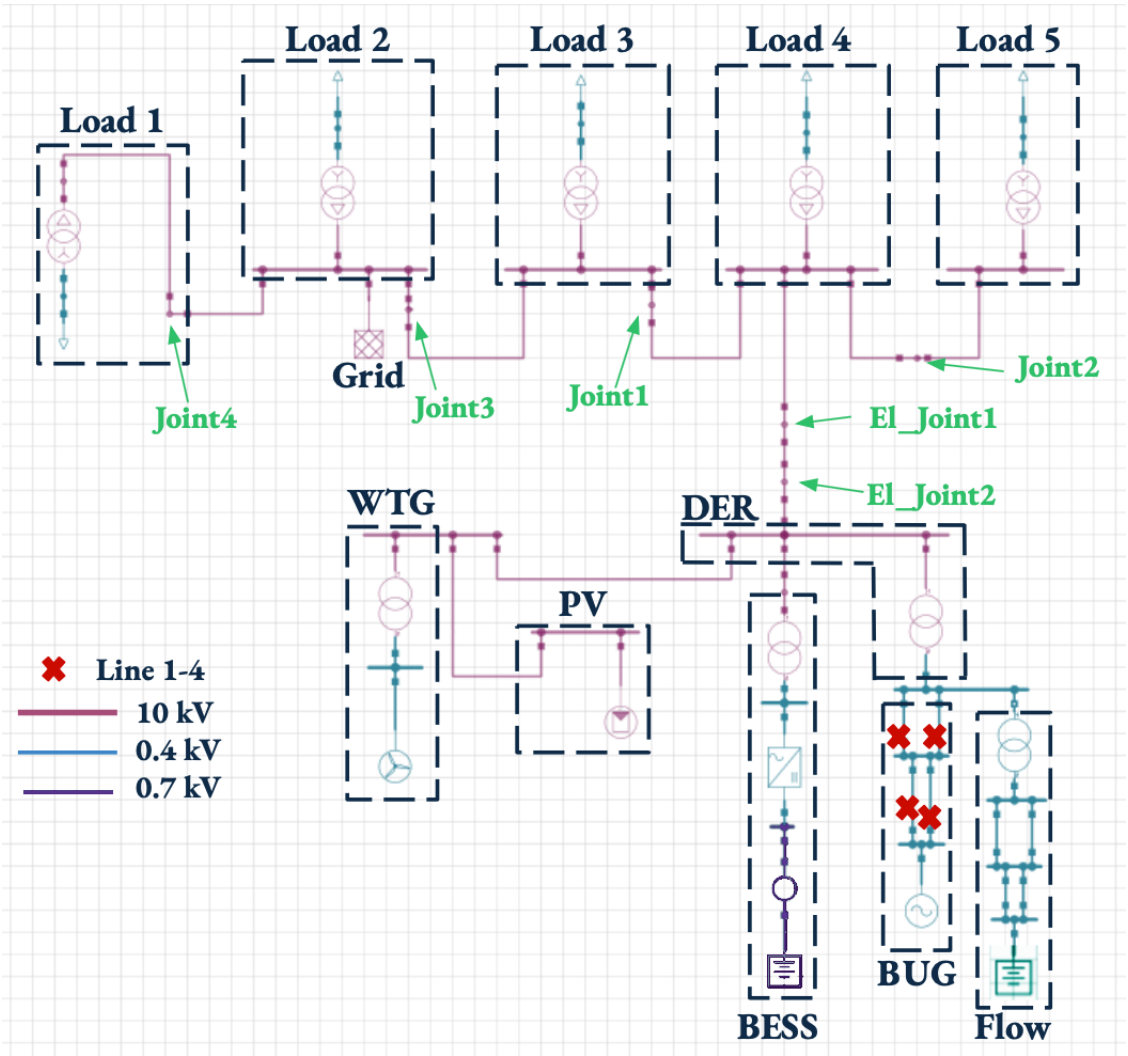

Figure 41: The model of the microgrid in NEPLAN where the distribution grid is connected. The pink lines represent the 10kV grid, the turquoise lines represent the 0.4 kV grid and the purple lines represent the 0.7kV grid. The red cross represent Line 1-4.

6.1.1 NEPLAN

NEPLAN is a software tool that can analyse, plan, optimise and simulate electrical networks. The software allows the user to conduct study cases very efficiently since it has a user-friendly graphical interface with comprehensive libraries [52]. For the case study examined in this thesis, NEPLAN was used to conduct harmonic analysis where the harmonic level for each frequency, frequency response and node could be determined [53]. NEPLAN uses equation 15 to calculate THD for voltage.

6.1.2 Components

Renewable energy source
A power source has to be modelled as AC to generate harmonics in the simulation program. For that reason, the WT and PV installation were both modelled as AC disperse generators instead of DC generators with their respective inverters. The AC disperse source was set to a harmonic source with current harmonic values from the on-site collected data. In table 19, in Appendix A, the values used for the WT and the PV installation are presented. The on-site harmonic data was used in the model. The power data connected to the PV installations was collected in X-PV, located on the MV side of the transformer. Thus, the PV-installation is connected directly to the MV grid in the model, and the rated voltage was set to 10 kV. See figure 41. The current harmonics from the PV were set with a 30°phase angle so that the harmonics from the WT and PV do not cancel each other. The difference in voltage harmonics when the current harmonics from PV are with and without phase angle will be presented in section 6.3.1.

BUG and BESS
The microgrid contains a BUG modelled as a synchronous machine following the technical specifications of the real generator, model GTS550GSA. The values for the Li-ion battery in BESS are a combination of default values from NEPLAN and data about the battery in Simris. The relevant active and reactive power on each side of the inverter was put in the model-based of collected data. The values used for the BUG and Li-ion battery are presented in table 20 and 21 in Appendix A. The flow battery was a later addition to the microgrid in Simris and not connected until March 2019. This was after the on-site data used in this thesis was collected therefore the flow battery is not connected to the rest of the microgrid in the model.

Transformers
All transformers in the microgrid transform voltage between 0.4 kV and 10 kV. The transformers used in the model were chosen from the NEPLAN library based on the known rated power. Transformer details are presented in table 22 in Appendix A. The transformer connecting BESS to the MV grid should be a three winding transformer, see figure 1 but was instead modelled as a two-winding transformer due to lack of component information and no library examples in NEPLAN. In a three-winding transformer, the third winding, which is delta, can cancel out the harmonics generated by the primary and secondary winding. However, BESS is not a source of harmonics in the model and therefore, the harmonic analysis results will not be affected.

Cables
The cables and their values that were used in the modelling were based on cable data provided by E.ON, which is presented in table 5. Several of the cables are short and the impedance is small, which means that the total resistance through the microgrid is small. The resistance between PV and Joint4 is 2.6 Ω. Having short cables with small impedance can cause convergence problems in NEPLAN.

Table 5: The cables used in the modelling of the Simris microgrid and their parameters. The resistance, reactance (at 50Hz) and capacitance are positive sequence values.

From	To	Type	Length (m)	Dimensions (mm^2)	R (Ω/km)	X (Ω/km)	C ($\mu F/km$)
DER	WTG.	AXLJ-TTCL TSLF	8.1	95/25	0.32	0.21	0.21
WTG	PV	AXLJ	35.1	50/16	0.641	0.11	0.23
DER	BESS	AXLJ-TTCL TSLF	38.8	95/25	0.32	0.21	0.21
Load 4	El_Joint1	Axclight-F LT	297.3	95/25*	0.32	0.10	0.32
El_Joint1	El_Joint2	AXLJ-F TTCL	1.3	95/25	0.32	0.122	0.32
El_Joint2	DER	AXLJ-TTCL TSLF	5.1	95/25	0.32	0.21	0.21
Joint2	Load 5	AXLJ-F LT	689.1	240/35	0.206	0.10	0.43
Load 4	Load 5	AXLJ	273.1	240/35	0.125	0.09	0.43
Load 3	Joint1	AXLJ-TTCL TSLF	3.9	240/35	0.125	0.19	0.30
Joint1	Load 4	AXCEL	796	240/35	0.125	0.085	0.40
Load 3	Joint3	AXLJ-TTCL TSLF	3.7	240/35	0.125	0.19	0.30
Joint3	Load 2	AXCEL	288.5	240/35	0.125	0.085	0.40
Load 2	Joint4	ACJJ	177.9	95	0.32**	0.097	0.33
Joint3	Load 1	AXCEL	753.9	50/16	0.641	0.11	0.24
Line 1-6		LV-4CA PPM AL***	10	150	0.207	0.083	0

*Dimension was assumed
**Resistance value was assumed.
***Cable type was assumed.

6.1.3 Assumptions

Following assumptions have been made about the simulation model:

- The system is balanced
- The only source of harmonics are the WT and PV installation.
- The PV installations rated voltage is set to 10 kV and connected to the MV grid.
- The current harmonics from the PV have a phase angle of 30 °.
- During island mode the BUG is connected and generates the missing power.
- During grid-connected mode the BUG is disconnected and the distribution grid provides the microgrid with extra power.
- The BESS is charged with the excess power from the WT and PV plant.
- The flow battery is disconnected.
- The BESS transformer is two winding.

6.1.4 Cases

Harmonic analysis was performed in NEPLAN in order to find the voltage THD and individual voltage harmonics at X-Load. The simulations were done on two different cases presented in table 6 below. The purpose of the different cases was to examine and compare how the model behaves under island mode and grid-connected mode compared to the actual microgrid.

Each case was examined under an interval of an hour, with six 10 minute interval values. For each 10-minute value, the average active- and reactive power for each load and production source was extracted from the collected data and set for the model. The current harmonics from both the WT and the PV plant seen in section 5 were used to set the two sources as harmonic sources.

Table 6: The cases that were simulated in NEPLAN, with the average active- and reactive power for all the loads. The average wind- and PV power that was generated under the interval are also presented.

Simulation cases						
Mode	**Date**	**Time**	**Avg.** P_{load}	**Avg.** Q_{load}	**Avg. Wind power**	**Avg. PV power**
Island	6 Nov. 2018	10-11	244.36 kW	49.87 kvar	142.19 kW	123.56 kW
Grid-connected	15 Oct. 2018	09-10	181.04 kW	29.95 kvar	180.53 kW	149.66 kW

6.2 Validation

To validate the model, a comparison to the collected data values was made in different nodes. A load flow validation was comparing the key quantities power and voltage. A harmonic analysis validation was also done to compare the following key quantities: phase angle, THD for voltage and RMS current. The validation was performed on the model in island mode as well as in grid-connected mode, for the first time interval in each case.

6.2.1 Load Flow Validation

In the load flow validation the following nodes were examined:

- X-Load
- X-PV
- X-El_Joint2
- X-GridPoint (only during grid-connected mode)

See figure 8 for reference.

In tables 7, 8, 9 and 10 the values for voltage, active- and reactive power are presented. Both the collected data and the power data used in the model are 10 min average values collected from the measurement tools. This can give an error as the values are not precise. In both X-PV and X-Load the differences for all variables are small, while the reactive power makes the big difference in both X-El_Joint2 and X-GridPoint. A theory for this is that there might be a capacitance in the filtering in the actual microgrid, which decreases the reactive power and as the model does not contain one, the reactive power becomes bigger for the simulated value than for the collected data value.

The difference in active power for X-El_Joint2 at grid-connected mode is because the BUG is assumed disconnected in this mode. However, it was connected in the actual grid and supplied a small amount of both active- and reactive power. Although the flow of reactive power in the model is admittedly the quantity with the worst match, both the simulated and measured values are fully realistic. Therefore the simulation model is considered valid.

Table 7: Power and voltage at X-Load, for both island mode and grid-connected mode.

	Island mode			Grid-connected mode		
	Collected data	**Model data**	**Difference**	**Collected data**	**Model data**	**Difference**
Active power	144.04 kW	144.04 kW	0 kW	119.74 kW	119.74 kW	0 kW
Reactive power	34.82 kvar	34.82 kvar	0 kvar	20.93 kvar	20.93 kvar	0 kvar
Voltage	0.405 kV	0.42 kV	0.015 kV	0.403 kV	0.43 kV	0.027 kV

Table 8: Power and voltage at the X-PV, for both island mode and grid-connected mode.

	Island mode			Grid-connected mode		
	Collected data	**Model data**	**Difference**	**Collected data**	**Model data**	**Difference**
Active power	140.19 kW	140.19 kW	0 kW	111.99 kW	111.99 kW	0 kW
Reactive power	3.31 kvar	3.31 kvar	0 kvar	2.76 kvar	2.76 kvar	0 kvar
Voltage	10.7 kV	10.66 kV	0.04 kV	10.63 kV	10.7 kV	0.07 kV

Table 9: Power and voltage at the X-El_Joint2, for both island mode and grid-connected mode.

	Island mode			Grid-connected mode		
	Collected data	**Model data**	**Difference**	**Collected data**	**Model data**	**Difference**
Active power	253.54 kW	252.3 kW	1.24 kW	215.48 kW	208.6 kW	6.9 kW
Reactive power	8.61 kvar	39.7 kvar	31.1 kvar	24.55 kvar	15.14 kvar	9.4 kvar
Voltage	10.75 kV	10.66 kV	0.09 kV	10.76 kV	10.7 kV	0.06 kV

Table 10: Power and voltage at X-GridPoint, for grid-connected mode.

Grid-connection point			
	Collected data	**Model data**	**Difference**
Active power	1.24 kW	1.22 kW	0.02 kW
Reactive power	22.44 kvar	31.84 kvar	9.4 kvar
Voltage	10.76 kV	10.7 kV	0.06 kV

6.2.2 Harmonic Analysis Validation

For the harmonic analysis validation, X-Load and X-PV were examined. The difference in phase angle, THD for voltage and RMS current for the two nodes are presented in table 11 and 12. The phase angle and RMS current were only compared for the fundamental frequency as data for the other harmonics were not available.

Table 11: Phase angle, THD of voltage and current at the X-Load, for island and grid-connected mode.

	Island mode			Grid-connected mode		
	Collected data	**Model data**	**Difference**	**Collected data**	**Model data**	**Difference**
Phase angle	14 °	14.02 °	0.02 °	15.64 °	10.35 °	5.29 °
U_{THD}	1.187 %	1.12 %	0.07%	1.45 %	0.94 %	0.51%
I_{RMS}	181.18 A	201.48 A	20.3 A	163.20 A	164.63 A	1.43 A

Table 12: Phase angle, THD of voltage and current at X-PV, for island and grid-connected mode.

	Island mode			Grid-connected mode		
	Collected data	**Model data**	**Difference**	**Collected data**	**Model data**	**Difference**
Phase angle	178.62 °	181.45 °	2.83 °	178.63 °	181.42 °	2.79 °
U_{THD}	1.34 %	1.12 %	0.22%	1.44 %	0.95 %	0.49 %
I_{RMS}	7.56 A	11.77 A	4.2 A	6.2 A	8.43 A	2.23 A

Current harmonics affect I_{RMS} which suggests that harmonics in the model are not equal to the harmonics from the collected data, as there is a difference in I_{RMS} for both cases. The voltage THD at both nodes in both cases is lower for the model. As THD depends on the individual harmonics, this also suggests that the model's harmonics are smaller than the harmonics from the collected data. The phase angles difference were small for each node in both cases. As both I_{RMS} and U_{THD} indicate differences in individual harmonics, the model is not valid for harmonic analysis.

6.3 Simulation Analysis

This section will present the results for the simulation cases. Simulated harmonic values will then get compared with the collected harmonic values. Furthermore, harmonics from X-Load will be suggested to get a more accurate model of the harmonics content and see if the difference can be minimized.

6.3.1 Simulation results

The two cases in table 6 converged in NEPLAN and the results are presented in table 13 for island mode and in table 14 for grid-connected mode. Both tables present the individual voltage harmonics and the voltage THD. Furthermore, the first time interval for each simulation was repeated when there was no phase angle on the harmonics produced by the PV. The results of this are presented in table 15.

Table 13: The results from simulation of the island mode case. The table shows each individual voltage harmonic and the voltage THD for each interval in time.

Time	**U H3**	**U H5**	**U H7**	**U H9**	**U H11**	**U H13**	**U H15**	U_{THD}
10:00	0 V	0.509 V	0.49 V	0 V	0.129 V	0.512 V	0 V	1.12 %
10:10	0 V	0.499 V	0.525 V	0 V	0.138 V	0.522 V	0 V	0.94 %
10:20	0 V	0.442 V	0.39 V	0 V	0.124 V	0.536 V	0 V	0.81 %
10:30	0 V	0.396 V	0.313 V	0 V	0.135 V	0.584 V	0 V	0.78 %
10:40	0 V	0.431 V	0.357 V	0 V	0.124 V	0.569 V	0 V	0.73 %
10:50	0 V	0.438 V	0.42 V	0 V	0.122 V	0.495 V	0 V	0.69 %

Table 14: The results from simulation of the grid-connected case. The table shows each individual voltage harmonic and the voltage THD for each interval in time.

Time	U H3	U H5	U H7	U H9	U H11	U H13	U H15	U_{THD}
09:00	0 V	0.959 V	1.004 V	0 V	0.393 V	0.946 V	0 V	0.94 %
09:10	0 V	0.961 V	1.063 V	0 V	0.395 V	0.976 V	0 V	0.98 %
09:20	0 V	0.985 V	1.007 V	0 V	0.52 V	0.814 V	0 V	1.47 %
09:30	0 V	1.102 V	0.986 V	0 V	0.534 V	0.800 V	0 V	1.65 %
09:40	0 V	1.195 V	1.072 V	0 V	0.49 V	0.88 V	0 V	1.41 %
09:50	0 V	1.217 V	1.065 V	0 V	0.47 V	0.92 V	0 V	1.23 %

Table 15: The results from the first time interval in each case when there was no phase angle on the PV harmonics. The table shows each individual voltage harmonic and the voltage THD.

Mode	U H3	U H5	U H7	U H9	U H11	U H13	U H15	U_{THD}
Island	0 V	0.377 V	0.274 V	0 V	0.095 V	0.382 V	0 V	0.65 %
Grid-connected	0 V	0.519 V	0.583 V	0 V	0.267 V	0.867 V	0 V	0.57 %

The individual harmonics are smaller when there is no phase angel on the PV harmonics, which indicates that the harmonics from the WT and PV-installation partially cancel each other out. As the THD also is smaller without phase angles, it suggests that having a 30 °phase angle is more accurate to the real microgrid. Therefore only the results from table 13 and 14 will be used for the comparison.

6.3.2 Comparison

In this section, the individual voltage harmonics and voltage THD will be analysed and compared with the collected values at X-Load. As the model is built on assumptions and average power values, it differs from the actual microgrid in Simris, which should be kept in mind when looking at the difference in results in this section. A more detailed comparison between every individual harmonic for both island and grid-connected mode is presented in figure 43 - 60 in Appendix B.

Individual harmonics
Figure 42 shows the simulated values in relation to the collected values for 3rd-15th harmonic in the X-Load. The simulated values(red) are generally smaller than the collected data values(blue) and the difference are shown in per cent in table 16. It can be seen that none of the simulated harmonics are similar in magnitude to the collected values.

The simulated and collected values are generally larger in grid-connected mode than in island mode as seen in when comparing figure 42a and 42b. This is probably due to the harmonics originating from outside the microgrid, as discussed before.

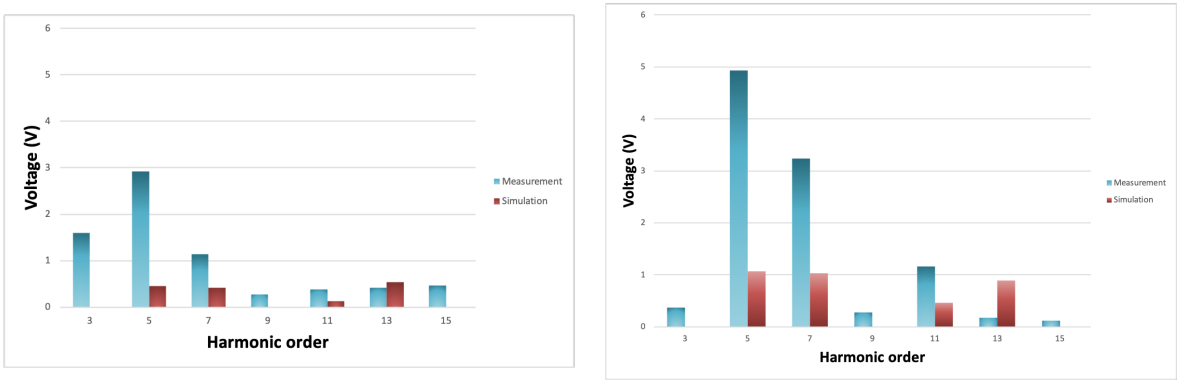

(a) Island mode

(b) Grid-connected mode

Figure 42: Individual voltage harmonics from the 3rd-15th order in X-Load where blue is the collected values and red the simulated values.

Table 16: Comparison of the average voltage harmonics and voltage THD for island mode and grid-connected mode between the collected and simulated values at X-Load.

	Island mode			**Grid-connected mode**		
Harmonic	**Collected data**	**Simulated**	**Difference**	**Collected data**	**Simulated**	**Difference**
3	1.6 V	0 V	1.6 V	0.36 V	0 V	0.36 V
5	2.92 V	0.45 V	2.47 V	4.93 V	1.07 V	3.87 V
7	1.14 V	0.42 V	0.73 V	3.24 V	1.03 V	2.21 V
9	0.28 V	0 V	0.28 V	0.27 V	0 V	0.27 V
11	0.38 V	0.13 V	0.25 V	1.17 V	0.47 V	0.7 V
13	0.41 V	0.54 V	0.12 V	0.17 V	0.89 V	0.72 V
15	0.46 V	0 V	0.46 V	0.12 V	0 V	0.12 V
U_{THD}	1.19 %	0.85 %	0.34 %	1.50 %	1.28 %	0.22 %

Triplen harmonics
The triplen harmonics are all zero in the simulations because the model is assumed to be balanced, meaning triplen harmonics got cancelled out by the delta connection in the transformers, as explained in section 3.1.2. The triplen from the collected data are nonzero, which suggests that the real microgrid is not balanced, as mentioned in section 5.

13th order harmonic
For both modes, one harmonic stands out from the rest and it is the 13th harmonic as it is the only harmonic where the simulated value is more significant than the measured value in the collected data. The main theory is that a harmonic filter was used in the microgrid to decrease 11th - or higher-order harmonics. The filter used in the Simris microgrid could be a damped filter which is commonly used for the 11th harmonic and above. The damped filter is a category of shunt filters that are rated for only part of the system voltage, making them a cost-efficient way of decreasing high-order harmonics, see section 3.1.5. As the model does not contain any harmonic filters, the 13th harmonic does not get cancelled out or decreased in the simulations.

THD
The voltage THD is larger for the collected microgrid data than for the simulated data, as the THD depends on the total amount of individual harmonics. There is a more significant difference in the values for island mode than for grid-connected mode, but the difference is unreasonably large for both cases.

The main reason for the difference in collected and simulated harmonic values is the assumption that only the WT and PV-plant produce harmonic emissions. It was shown in section 5 that there were harmonics in the microgrid from other sources as the distribution grid, inverters and loads. With this knowledge in mind, an additional harmonic source was added to represent the missing harmonics to improve the model and achieve a minimum difference. This is presented in the next section.

6.3.3 Load Harmonics

As seen in the previous section, the simulated harmonic values were not similar to the collected harmonic values. In this section, current harmonics will be added to a load in the model to examine if the collected values can be reached and if the current harmonics added are reasonable. This was examined for the first time interval in each case.

X-Load was converted to a harmonic source to represent the missing harmonic emissions and the result is presented in table 17. It can be seen that all voltage harmonics during both cases could reach the collected data values except the 13th harmonic as it was already larger in the first place, see table 16 in the previous section.

The THD at X-Load became 1.4% for island mode and 1.58% for grid-connected mode, meaning that the THD became much higher than the measured value. Even if THD is within the 8%, limit according to table 2, the large values suggests that adding current harmonics to one load will not make the model valid for harmonics analysis.

Table 17: The needed current harmonics, Simulated I_h, from the load at X-Load for the voltage harmonics, Simulated U_h, to reach the voltage harmonics of the collected data, Collected U_h. The measurements were done for both island mode and grid-connected mode.

	Island mode			**Grid-connected mode**		
Harmonic	**Collected U_h**	**Simulated U_h**	**Simulated I_h**	**Collected U_h**	**Simulated U_h**	**Simulated I_h**
3	1.485 V	1.483 V	0.054 A	0.454 V	0.454 V	0.016 A
5	2.903 V	2.908 V	14.6 A	4.425 V	4.42 V	15.1 A
7	1.34 V	1.34 V	2.9 A	3.03 V	3.04 V	5.95 A
9	0.219 V	0.222 V	0.008 A	0.187 V	0.18 V	0.007 A
11	0.518 V	0.523 V	1.32 A	1.429 V	1.427 V	2.24 A
13	0.346 V	0.512 V	– *	0.138 V	0.946 V	– *
15	0.323 V	0.321 V	0.012 A	0.113 V	0.116 V	0.004 A

*No current harmonic placed at X-load.

To see if the current harmonics added at X-Load are reasonable, the magnitude in percentage for each current harmonic has been calculated and presented in table 18. By comparing the results of this table to the magnitudes in table 3 it can be seen that the 5th, 7th and 11th harmonic in grid-connected mode are above the average values for a residential area. Therefore adding load harmonics at one load in the model cannot solely make the model accurate to the actual grid.

Table 18: The magnitude for both island- and grid-connected mode, of the individual current harmonics, 3rd-15th, presented in table 17.

	Magnitude	
Harmonic	**Island**	**Grid-connected**
3	0.03 %	0.01 %
5	6.83 %	8.61 %
7	1.36 %	3.39 %
9	0.004 %	0.004 %
11	0.62 %	1.28 %
13	0.00 %	0.00 %
15	0.006 %	0.002 %

7 Conclusions

In this part conclusions about the research questions are made and future work is discussed.

This case study has shown that there is generally no relation between weather and harmonic emissions from wind power and solar power generation. Even if the power generated correlates with wind speed and irradiation, the current harmonics are on a constant level, except for the 5th harmonic from solar power during grid-connected mode. It is also seen that the current emissions are close to zero when there is no generation.

The harmonic emissions from the WT and the PV-panels are not the only harmonics seen in the microgrid and they are not the largest contribution to the harmonic emission in the grid. Generally, the voltage THD is approximately 2 % , but without generation from RES, the harmonic level is between 1.2-1.8 %. The majority of harmonic emissions seen in the grid are most likely originating from other sources in the microgrid or from the distribution grid. When comparing the harmonic emission levels in the microgrid with the EIFS 2013:1 regulations, the harmonic levels are far below the requirements and are at this point not at harmful levels. However, if more sources of harmonics were added to the grid in the future, this could potentially be a problem.

There was less difference than expected between harmonics when the system was connected to the distribution grid or in island mode. The harmonic levels were lower in island mode than in grid-connected mode, probably because of the disappearance of harmonic emission originating from the distribution grid. During grid-connected mode, harmonics from other sources connected to the distribution grid appear in the Simris microgrid, as harmonics can travel far. It is also possible that those harmonics are due to the disconnecting of BUG. The BUG is just used during island mode and can extinguish harmonics in the network. It would be interesting to look at the correlation between the harmonics and the BUG and between harmonics and load patterns.

The model validation showed that the key quantities voltage, active and reactive power were all valid, meaning that the model had a valid load flow compared to the real microgrid. For validation of harmonic analysis, the key quantities voltage THD and RMS current deviated from the collected data, indicating that the model is not valid for harmonic analysis. It also suggested that the model harmonics were smaller in magnitude to the collected data harmonics, which was then proven in the comparison of individual harmonics. It has been shown that a large amount of the harmonics result from other sources within the grid, so the assumption that WT and PV were the only sources of harmonics affected the validation and simulation result negatively. This was also seen when X-Load was remodelled into a harmonic source, and the simulated harmonics became similar to the collected values. So more work needs to be done to get a valid microgrid model in NEPLAN when analysing harmonic emissions, which will be discussed in future work.

7.1 Future Work

To get a valid model for harmonic analysis, some improvements have to be made. Harmonic data from all potential harmonic sources must be analysed and added as a harmonic source in the model. This includes the harmonic emission from the customer assets, the distribution grid, and the inverter connected to the battery. Further work on the model, such as examining the impedance and frequency dependence and finding information about the different components, could also minimise the number of assumptions and get a more accurate model. Furthermore, the BUG representation in the model should be investigated to examine its effect on harmonics when switching between the two modes.

More collected data during grid-connected and island mode should be analysed for different weather scenarios to get more reliable results. The probability of having a certain harmonic level could be studied

for a large amount of data to get a deeper analysis or using principal component analysis (PCA) or other data analysis methods. The harmonic emission spectra from the WT and PV could be studied to separate primary and secondary emissions. Additional parameters and all phases should also be examined in more nodes in the microgrid. The harmonic impedance for different harmonics and how they are affected when the system is in island mode is also an interesting viewpoint to examine. Furthermore, a higher frequency span could be studied to examine harmonics from components in the microgrid with a higher switching frequency.

This thesis has focused on a specific LES implemented by E.ON and the results are mainly representative of the microgrid in Simris. A logical next step would be to repeat this process and analysis for other microgrids.

It has been seen in this project and in previous projects that the harmonic levels do not correlate with power. To gain a deeper understanding of harmonics from RES, multiple different scenarios should be examined. Do several small installations result in increased harmonic compared to a single large one? Do installations from different manufactures with different harmonic spectra versus the same manufacture affect the harmonic content? As discussed above, there are many interesting future works addressing the subject of harmonics and microgrids.

References

[1] European Commission. *Clean Energy*. Jan. 2021. [Online]. URL: https://ec.europa.eu/international-partnerships/sdg/clean-energy_en.

[2] E.ON Energidistribution. *Microgrid drivers*. [Internal information]. 2019.

[3] N. Hancock. Private communication. Feb. 2021.

[4] S. Sahoo. *Elkvalitetsarbete i Sverige 2019 -En Studie av nuvarande arbetssätt och framtida utmaningar*. Feb. 2021. [Online]. URL: https://energiforsk.se/media/27406/elkvalitetsarbete-i-sverige-2019-energiforskrapport-2019-633.pdf.

[5] M. Bollen and I. Gu. *Signal Processing of Power Quality Disturbances*. John Wiley and Sons, Inc, 2006. ISBN: 9780471731689.

[6] Infrastrukturdepartementet RSED E. *Ellag 1997:857*. Feb. 2021. [Online]. URL: https://www.riksdagen.se/sv/dokument-lagar/dokument/svensk-forfattningssamling/ellag-1997857_sfs-1997-857.

[7] E.ON. *E.ON implements a stand-alone grid solution in Sweden*. 2017 [Online]. URL: https://www.eon.com/en/about-us/media/press-release/2017/eon-implements-a-stand-alone-grid-solution-in-sweden.html (visited on 01/12/2021).

[8] E.ON Energidistribution. *Simris – Grid topology and components*. [Internal information]. 2020.

[9] Y. Hayashi N. Kanao and J. Matsuki. "Analysis of Even Harmonics Generation in an Isolated Electric Power System". In: *Electrical Engineering in Japan* 167.2 (2009).

[10] Jakob Nömm, Sarah Rönnberg, and Math Bollen. "Harmonic voltage measurements in a single house microgrid". In: *2018 18th International Conference on Harmonics and Quality of Power (ICHQP)*. 2018, pp. 1–5. DOI: 10.1109/ICHQP.2018.8378921.

[11] S. Hansen L. Asiminoaei and F. Blaabjerg. "Predicting Harmonics by Simulations. A Case Study for High Power Adjustable Speed Drives". In: *Electrical Power Quality and Utilisation, Magazine* 2.1 (2006), pp. 65–75.

[12] M. Bollen and K. Yang. "Harmonic aspects of wind power integration". In: *Journal of Modern Power Systems and Clean Energy* 1 (June 2013), pp. 14–21.

[13] M. Bollen and D. Schwanz. *HARMONICS AND WIND POWER*. Tech. rep. 469. Energiforsk AB. Luleå university of technology, 2018.

[14] K.Yang. "On Harmonic Emission, Propagation and Aggregation in Wind Power Plants". PhD thesis. Department of Engineering Sciences and Mathematics. Luleå University of Technology, Skellefteå 2015.

[15] K. Dartawan et al. *Harmonics issues that limit solar photovoltaic generation on distribution circuits*. Tech. rep. Albany, NY, USA: Pterra Consulting, LLC, 2012.

[16] S. Rönnberg. “Emissions and interaction from domestic installations in low voltage electricity network, up to 150 kHz”. PhD thesis. Department of Engineering Sciences and Mathematics. Luleå University of Technology, Luleå 2013.

[17] N. Hatziargyriou et al. “Microgrids”. In: *IEEE Power and Energy Magazine* 5.4 (2007), pp. 78–94.

[18] X. Li, Y-J. Song, and S-B. Han. “Frequency control in micro-grid power system combined with electrolyzer system and fuzzy PI controller”. In: *Journal of Power Sources* 180.1 (2008), pp. 468–475.

[19] J. A. P. Lopes, C. L. Moreira, and A. G. Madureira. “Defining control strategies for MicroGrids islanded operation”. In: *IEEE Transactions on Power Systems* 21.2 (2006), pp. 916–924.

[20] Sunmodule. *SW 245 poly / Version 2.0 and 2.5 Frame*. SW-02-5009US 01-2012 US. March 2012. [Online].

[21] SMA Solar Technology AG. *Sunny Tripower 10000TL/12000TL/15000TL/70000TL*. STP10-17TL-IA-en-32 Verison 3.2. 2013.

[22] S.Surawdhaniwar and R. Diwan. “Study of Maximum Power Point Tracking Using Perturb and Observe Method”. In: *International Journal of Advanced Research in Computer Engineering Technology* 1.5 (July 2012), pp. 106–110.

[23] E.ON Energidistribution. *WINDTEST KWK GmbH*. Nov. 2001 [Internal information].

[24] ENERCON. *ENERCON wind energy converter. Technology and Service*. June 2015.

[25] Enerox. *Appendix C: Technical Brochure. System Documentation CellCube FB 250 R3*. May 2018 [Internal information].

[26] O. Ivarsson. Private communication. Apr. 2021.

[27] Metrum. *Tekniska specifikationer*. 2021. [Online]. URL: `https://metrum.se/sv/produkt/metrum-sc/` (visited on 03/26/2021).

[28] Janitza electronics GmbH. *Power Quality Analyser UMG 605-PRO - User manual and technical data*. 2020. [Online].

[29] M. Bollen. *Understanding Power Quality Problems: Voltage Sags and Interruptions*. John Wiley and Sons, 2000. ISBN: 0-7803-4713-7.

[30] G. Morén. “EIFS 2013:1 Energimarknadsinspektionens föreskrifter och allmänna råd om krav som ska vara uppfyllda för att överföringen av el ska vara av god kvalitet”. In: *Energimarknadsinspektionens författningssamling* (2013). ISSN: 2000-592X.

[31] S. V. Rode and S. A. Ladhake. “Analysis and Technique for Harmonics Elimination from periodic waveform”. In: *IEEE-International Conference On Advances In Engineering, Science And Management (ICAESM -2012)*. 2012, pp. 596–600.

[32] E.H. Mayoral et al. “Fourier Analysis for Harmonic Signals in ElectricalPower Systems”. In: *IntechOpen: Fourier Transforms High-tech Application and Current Trends* (2017).

[33] M. F. Abdullah et al. “The study of triplen harmonics currents produced by salient pole synchronous generator”. In: *Proceedings of the 2011 International Conference on Electrical Engineering and Informatics*. 2011, pp. 1–5.

[34] M. Grady. “Understanding Power System Harmonics”. In: University of Texas at Austin, 2012. Chap. 1.

[35] Circuit Global. *Harmonics in Three Phase Transformers*. Mar. 2021. [Online]. URL: `https://circuitglobe.com/harmonics-in-three-phase-transformers.html`.

[36] M. de Apráiz J. Barros and R. I. Diego. “Investigation of even harmonics in low-voltage distribution networks”. In: *2020 IEEE International Instrumentation and Measurement Technology Conference (I2MTC)*. 2020, pp. 1–6.

[37] O. Samuelsson. Private communication. Lunds Teckniska Högskola. Maj 2021.

[38] L. Piegari S. D’Arco and P. Tricoli. “Harmonic compensation with active front-end converters based only on grid voltage measurements”. In: *3rd Renewable Power Generation Conference (RPG 2014)*. 2014, pp. 1–6.

[39] S. M. Halpina and A. Card. “Power Electronics Handbook”. In: Butterworth-Heinemann, 2011. Chap. 40.

[40] J.K. Phipps, J.P. Nelson, and P.K. Sen. “Power quality and harmonic distortion on distribution systems”. In: *IEEE Transactions on Industry Applications* 30.2 (1994), pp. 476–484.

[41] D. Shmilovitz. “On the Definition of Total Harmonic Distortion and Its Effect on Measurement Interpretation”. In: *IEEE TRANSACTIONS ON POWER DELIVERY* 20.1 (2005), pp. 526–528.

[42] I.V. Blagouchine and E. Moreau. “Analytic Method for the Computation of the Total Harmonic Distortion by the Cauchy Method of Residues”. In: *IEEE TRANSACTIONS ON COMMUNICATIONS* 59.9 (2013), pp. 2478–2491.

[43] A. Rashid. “Harmonic load flow formulation and numerical resolution”. PhD thesis. Barcelona, Spain: Universitat Politecnica de Catalunya, 2012.

[44] IEEE Power Engineering Society Harmonics Working Group. *Tutorial on Harmonics Modeling and Simulation*. IEEE Power Engineering Society. Piscataway, NJ, USA, 1998.

[45] D. D. Morton. “Impact of System Impedance on Harmonics Produced by Variable Frequency Drives (VFDs)”. MA thesis. Virginia Polytechnic Institute and State University, 2015.

[46] M. Bollen. Private communication. Luleås Tekniska Universitet. Apr. 2021.

[47] M. Bollen and S. Rönnberg. “Primary and secondary harmonics emission; harmonic interaction - a set of definitions”. In: *2016 17th International Conference on Harmonics and Quality of Power (ICHQP)*. 2016, pp. 703–708.

[48] S. T. Tentzerakis and S. A. Papathanassiou. “An Investigation of the Harmonic Emissions of Wind Turbines”. In: *IEEE Transactions on Energy Conversion* 22.1 (Feb. 2007), pp. 150–158.

[49] S. Rönnberg, M. Bollen, and A. Larsson. "Grid impact from PV-installations in Northern Scandinavia". In: *22nd International Conference and Exhibition on Electricity Distribution (CIRED 2013)*. Stockholm, Sweden, 2013, pp. 1–4.

[50] P. G. Salomé E. M. V. Filho M. M. Ribeiro and P. F. Ribeiro. "Influence of harmonic distortion in current transformer". In: *2016 17th International Conference on Harmonics and Quality of Power (ICHQP)*. 2016, pp. 599–604.

[51] D. Eriksson. "Utredning om förekomsten och inverkan av övertoner i Umeås centrala elnät". MA thesis. Umeå University, 2013.

[52] NEPLAN. *Electricity*. Feb. 2021. [Online]. URL: https://www.neplan.ch/neplanproduct/en-electricity/.

[53] NEPLAN. *Harmonic Analysis*. Feb. 2021. [Online]. URL: https://www.neplan.ch/description/harmonic-analysis-2/.

Appendix

A Component values in NEPLAN

In this appendix the values and types used for the different components in NEPLAN are presented. In table 19 the values used for the WTG and PV generator are shown, in 20 the values for the BUG are shown and in table 21 the values used for the BESS are shown. The different transformers used and their rated powers and vector groups are presented in table 22.

Table 19: The values used for the wind turbine generator and PV generator.

	Wind turbine	**PV Plant**
Rated voltage (kV)	0.4	0.4
Rated power (kVA)	500	440
Rated power factor	0.89	1
Input current (A)	721.7	635.1
Flicker coefficient	6	-

Table 20: The values used for the BUG in NEPLAN.

Backup Generator	
Rated voltage (kV)	0.4
Rated power (kVA)	550
Rated current (A)	792
Power factor	0.8
Engine Revs (rpm)	1500

Table 21: The values used for the BESS in NEPLAN.

Lithium-Ion battery	
Voltage setpoint (V)	787.2
Number of cells per tray	16
Number of tray per series string	12
Number of parallel strings	7
Values below are per tray	
Rated voltage (V)	65.6
Rated current (A)	0.25
Internal series resistance* (Ω)	0.1
Rated capacity (Ah)	68
Nominal voltage (V)	58.4
Polarization constant* (V/Ah)	0.047
Exponential zone amplitude* (V)	4.75596
Exponential zone time constant inverse* (1/Ah))	26.5487

*Default value from NEPLAN

Table 22: The values and names for the transformers used in the simulations, which all transformed voltage between 0.4kV and 10kV.

Location	Type	Rated power (kVA)	Vector group
WTG Station	DIN 42500 (Oil) 630kVA	500	Dyn5
BESS	DIN 42500 (Oil) 800kVA	800	YNd5
DER	DIN 42500 (Oil) 630kVA	630	Dyn5
Load 5	DIN 42500 (Oil) 400kVA	400	Yd5
Load 4	DIN 42500 (Oil) 100kVA	100	Yd5
Load 3	DIN 42500 (Oil) 400kVA	315	Yd5
Load 2	DIN 42500 (Oil) 630kVA	500	Yd5
Load 1	DIN 42500 (Oil) 100kVA	100	Yd5

B Measurement data vs simulation data

In this Appendix the measurement and simulation value for each individual voltage harmonic are presented to get a more detailed comparison. Furthermore the voltage THD of the two is also presented. Each comparison is presented as a function of both wind speed and irradiation.

B.0.1 Island Mode

In this section the results for the measurement values during island mode are compared with the simulation values from the same case. In figures 43 to 46 the individual harmonics are presented as a function of wind speed, whilst in figures 47 to 50 they are presented as a function of irradiation. The voltage THD is presented in figure 51.

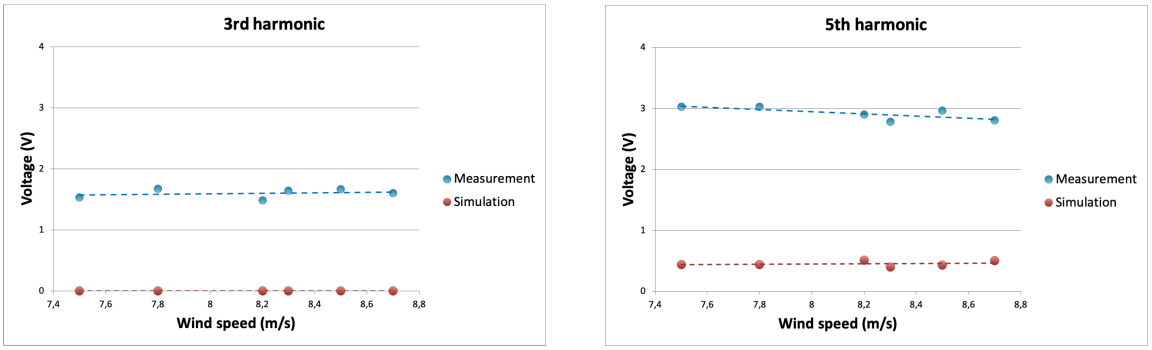

Figure 43: 3rd and 5th voltage harmonic from the measurement values, blue, and the simulated values, red, in island mode.

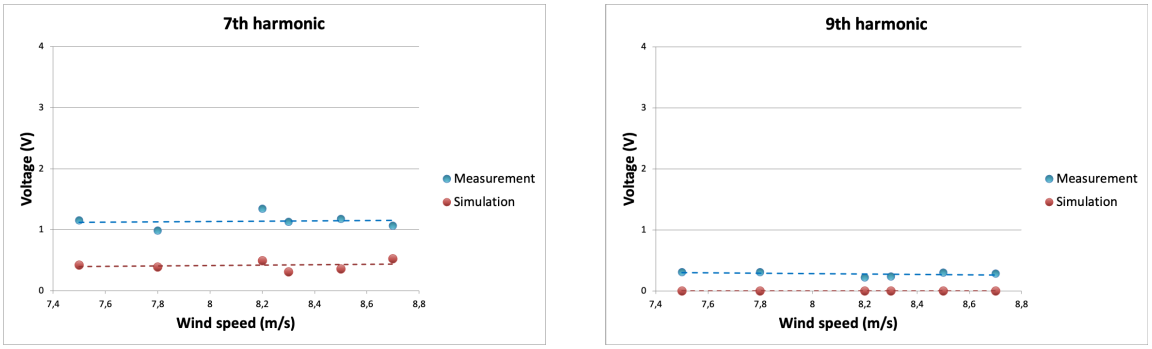

Figure 44: 7th and 9th voltage harmonic from the measurement values, blue, and the simulated values, red, in island mode.

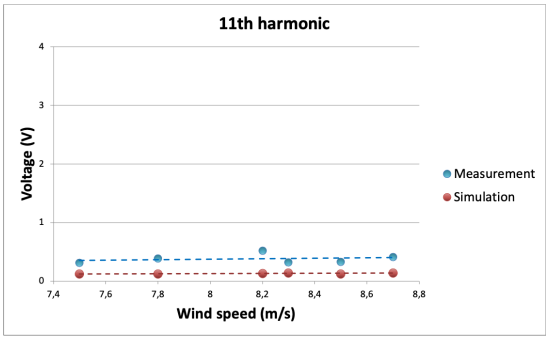

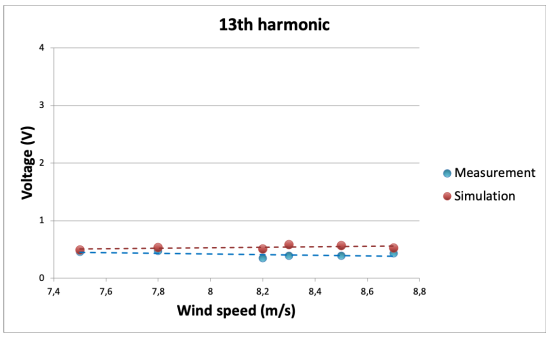

Figure 45: 11th and 13th voltage harmonic from the measurement values, blue, and the simulated values, red, in island mode.

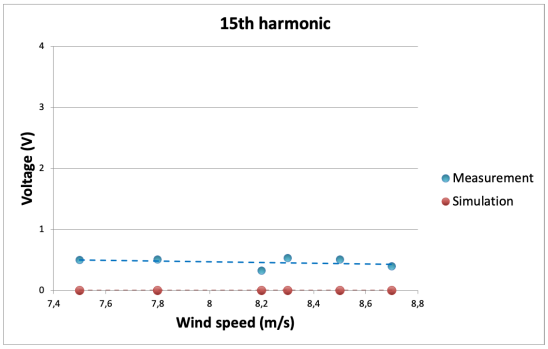

Figure 46: 15th voltage harmonic from the measurement values, blue, and the simulated values, red, in island mode.

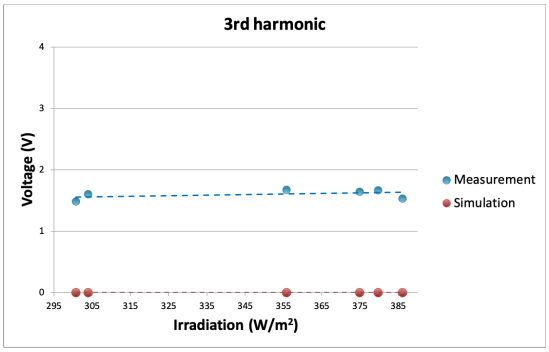

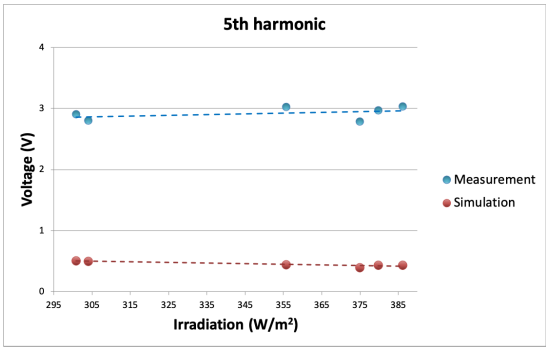

Figure 47: 3rd and 5th voltage harmonic from the measurement values, blue, and the simulated values, red, in island mode.

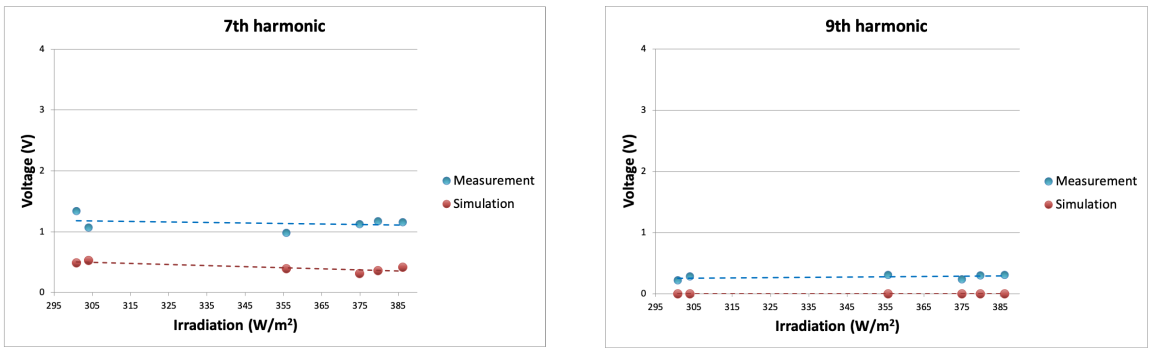

Figure 48: 7th and 9th voltage harmonic from the measurement values, blue, and the simulated values, red, in island mode.

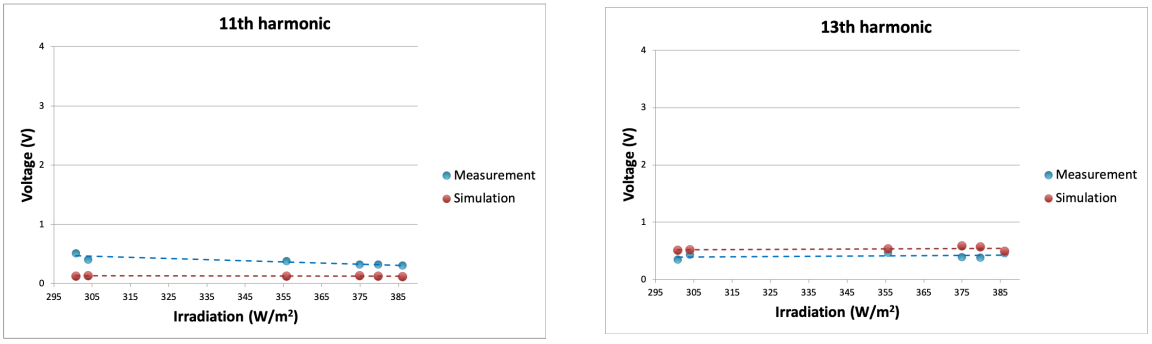

Figure 49: 11th and 13th voltage harmonic from the measurement values, blue, and the simulated values, red, in island mode.

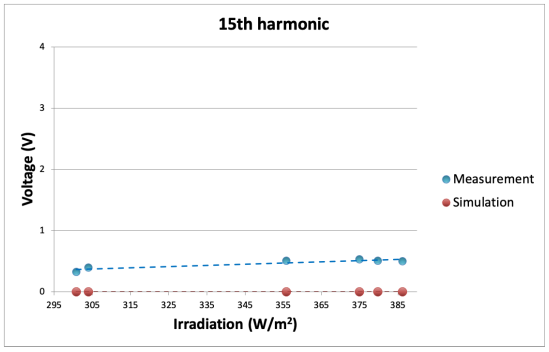

Figure 50: 15th voltage harmonic from the measurement values, blue, and the simulated values, red, in island mode.

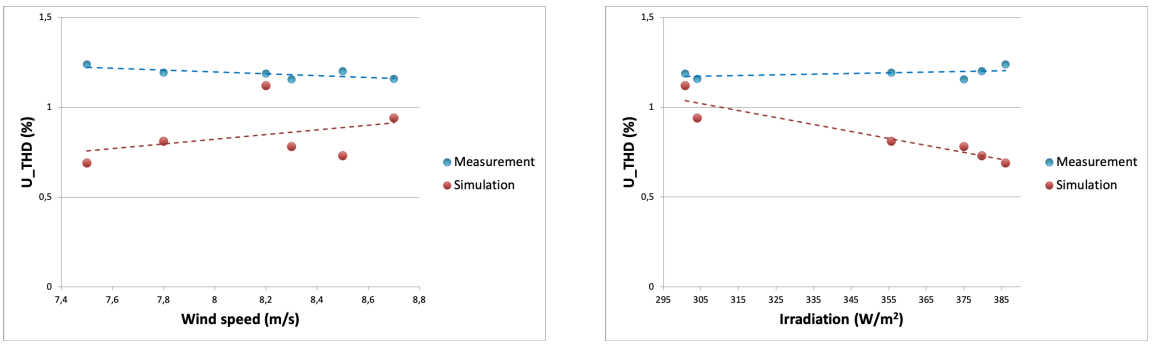

Figure 51: Voltage THD from the measurement values, blue, and the simulated values, red, in island mode.

B.0.2 Grid-Connected Mode

In this section the results for the measurement values during grid-connected mode are compared with the simulation values from the same case. In figure 52 to 55 the individual harmonics are presented as a function of wind speed, whilst in figure 56 to 59 they are presented as a function of irradiation. The voltage THD is presented in figure 60.

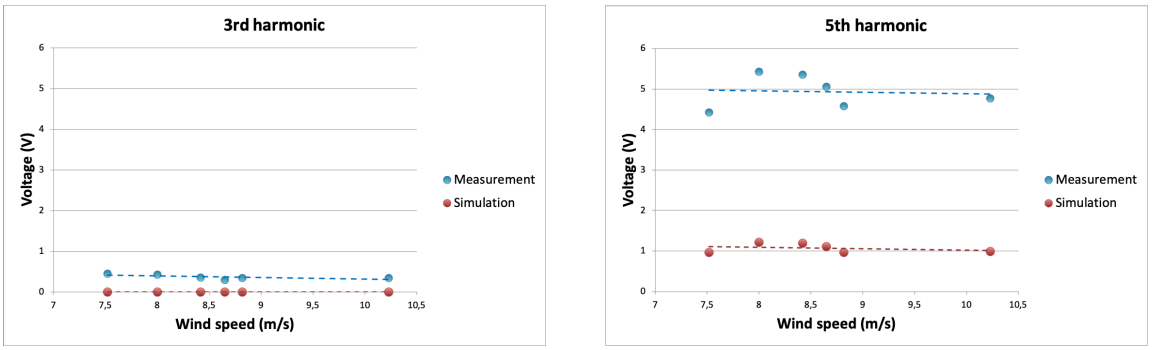

Figure 52: 3rd and 5th voltage harmonic from the measurement values, blue, and the simulated values, red, in grid-connected mode.

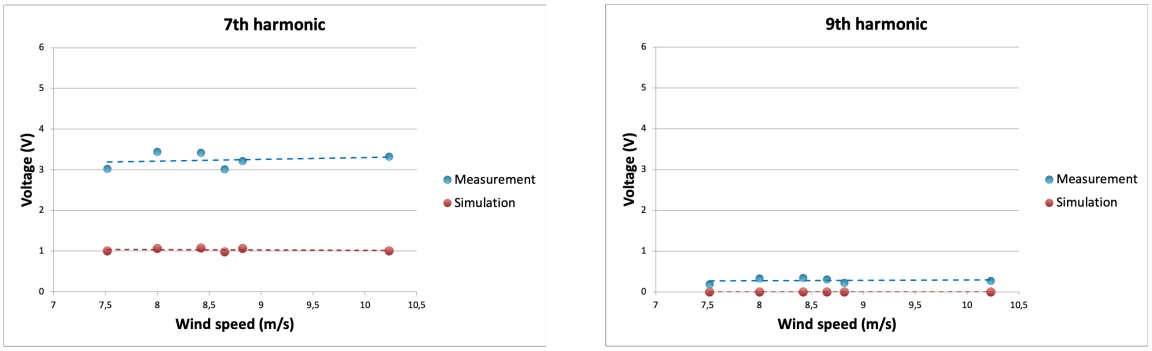

Figure 53: 7th and 9th voltage harmonic from the measurement values, blue, and the simulated values, red, in grid-connected mode.

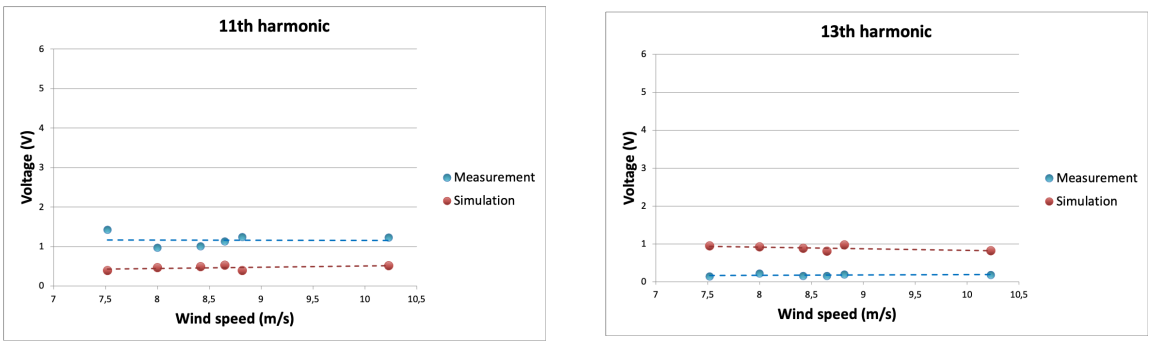

Figure 54: 11th and 13th voltage harmonic from the measurement values, blue, and the simulated values, red, in grid-connected mode.

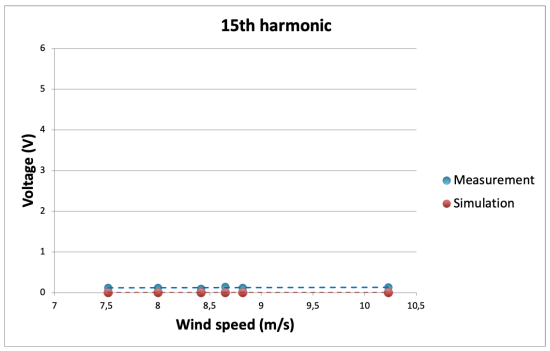

Figure 55: 15th voltage harmonic from the measurement values, blue, and the simulated values, red, in grid-connected mode.

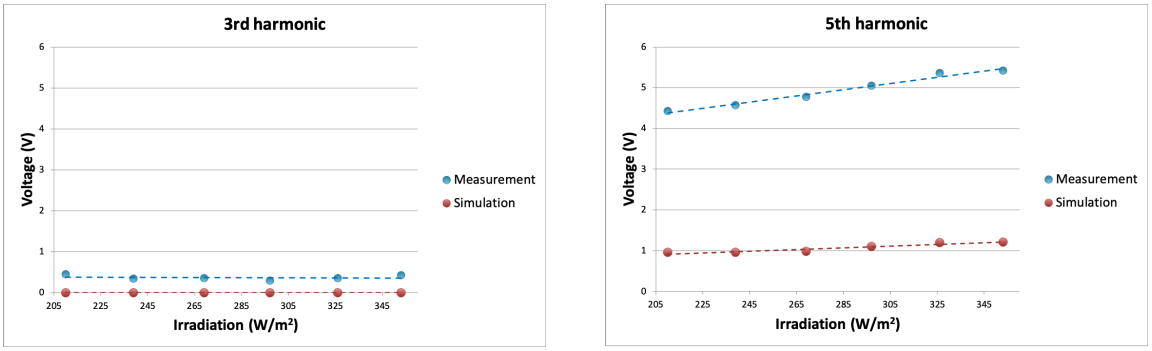

Figure 56: 3rd and 5th voltage harmonic from the measurement values, blue, and the simulated values, red, in grid-connected mode.

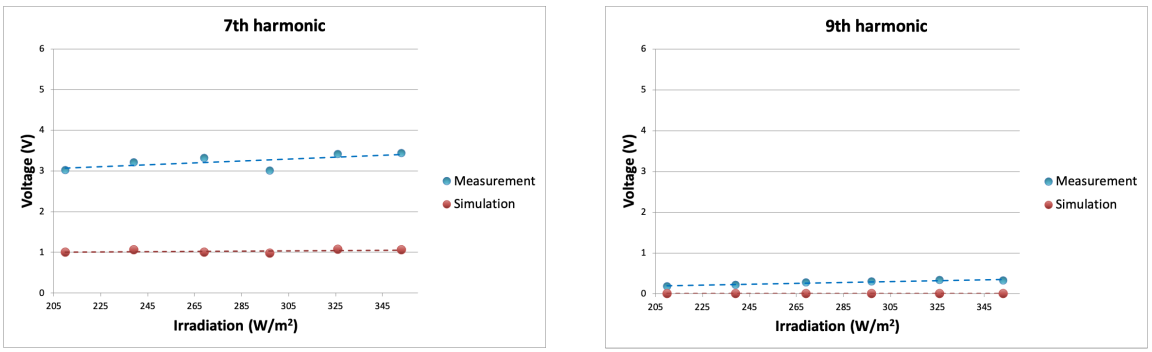

Figure 57: 7th and 9th voltage harmonic from the measurement values, blue, and the simulated values, red, in grid-connected mode.

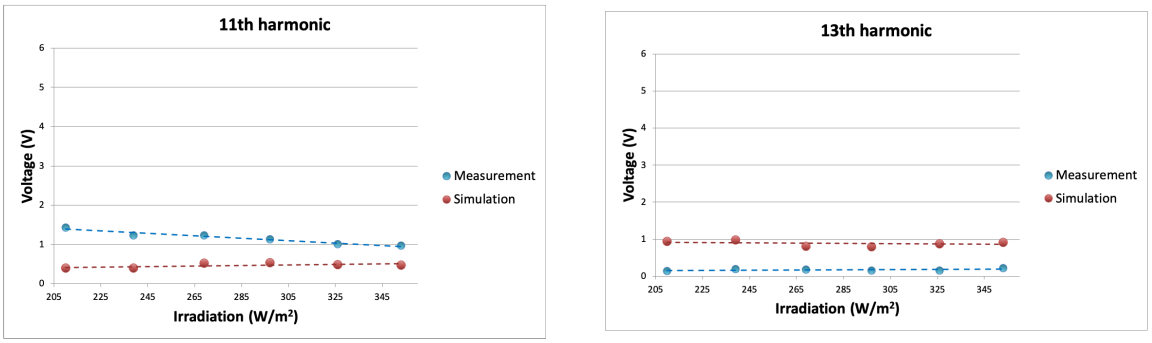

Figure 58: 11th and 13th voltage harmonic from the measurement values, blue, and the simulated values, red, in grid-connected mode.

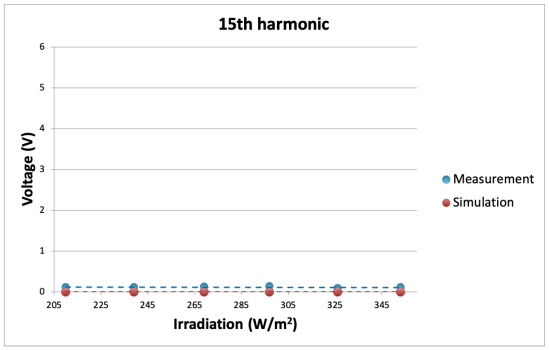

Figure 59: 15th voltage harmonic from the measurement values, blue, and the simulated values, red, in grid-connected mode.

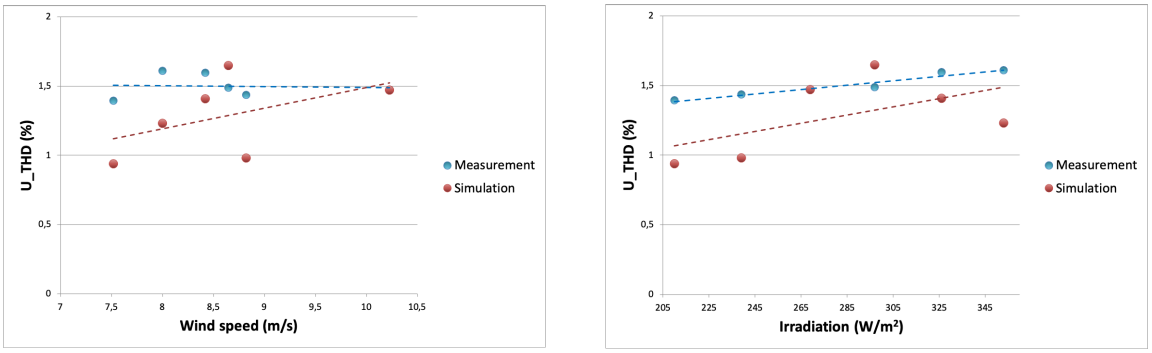

Figure 60: Voltage THD from the measurement values, blue, and the simulated values, red, in grid-connected mode.